Projet LEZ 2020 Cofinancé par le fonds Européen au Développement Régional

HADES: DESIGN AND MODELLING OF AN UNDERWATER EEL-LIKE ROBOT

Presented by: Elio Jabbour

Supervisor: Dr. Lionel Lapierre

Reviewer: Dr. Olivier Strauss

21 February,2022

I. Table of Contents

II. Table of Figures

III. Introduction

Underwater vehicles have carried out subsea operations and missions that are too dangerous for the human intervention. As the technology has progressed throughout the years, bionics is becoming the latest trend since most of the complex engineering answers hides in the life form on this planet. This paper introduces Hades, the underwater snake robot that is getting ready for the exploration of the underworld. Karst systems remains a mystery for explorers and answers for geologist who seeks data and whether the water that exists under land could help urban development and a better sustainable environment. This paper will give a brief introduction in these matters as well as try to find a solution by introducing Hades with a design, modelling, numerical simulations and thruster configuration study to show whether this system has the rightful and valid claim to be the god of the underworld.

Karsts and alternatives water resources were the fundamental requirements for civilizations to have a primitive development. Because of the shortage of water surface flows, it has become necessary for cities to rely on water supplied by karst springs. Throughout the time, it was the Phoenician civilization (modern age's Lebanon) that invented the aqueducts that has brought a great advantage for cities to have water supplies transportation from the main water resource. Thanks to the formation of karts, it has brought a great role to Engineering and geosciences, other than its fresh water storage, karsts are the biggest contributors as a carbon sink and as historical climate records. However, they offer a serious hazard for urban development since they can create unpredictable land surface collapse, sinkhole flooding which results in urban damages on grand scale. It should also be noted that without careful planning of urban development, water pollution could contaminate these karsts and damage the biological environment [**1**].

By definition karts, Karst is a topography formed from the dissolution of soluble rocks such as limestone, dolomite, and gypsum. It is characterized by underground drainage systems with sinkholes and caves [**2**]. The characteristics of karts includes the following: (a)internal drainage of surface runoff through sinkholes, (b)underground diversion of surface streams, (c)storage of water known as *epikarst zone*, (d)rapid flow though pipelike surfaces called *conduit*(e)discharge of water by one or more large perennial springs. Figure (**1)** illustrate the features of a well-developed karst.

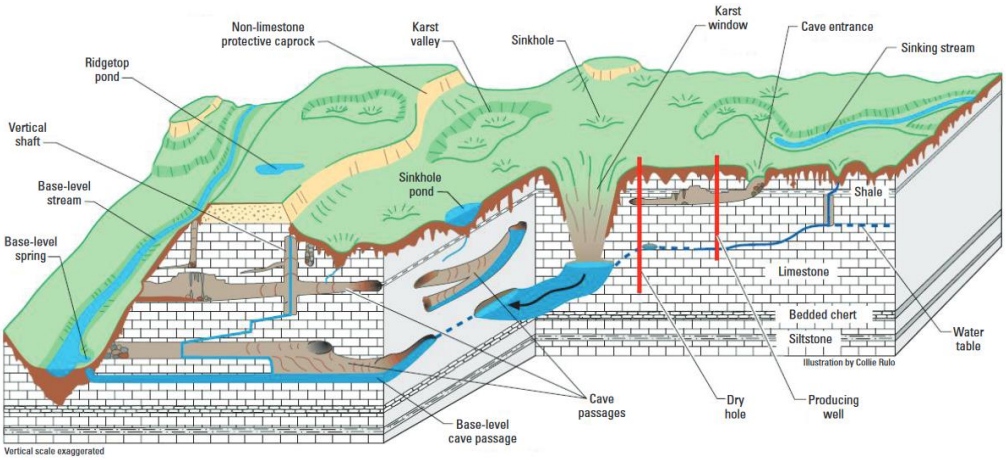

*Figure 1 Physiographic and hydrologic features typical of a well-developed karst terrane, Kentucky Geological Survey [**3**]*

IV. Literature Review

Fontaine de Vaucluse, located in southern France, was one of the first documented reports about underwater robotics teleoperation in caves exploration where the *Telenaute* ROV (Remotely Operated Vehicle) managed to reach 106 meters of depth in 1967.However, this cave has witnessed a history of turnaround ever since and fascinatingly the Renault funded ROV *Sorgonaute*,1983, managed to reach 243 meters due to the max cable length, surprisingly the upgraded version of *Sorgonaute* in the following year managed to reach less depth and was trapped along a lifeline. This motivated the next 2 missions of 1986 and 1988 to rescue this lost lonely drone but they ended up again as a failure of their own existence. Few questions were arisen at the time whether the *design* or the *methods* of using such technique is right for this type karst caves exploration. The answer came later in 1989, when Spelenaute, by COMEX, won its reputation when it reached the terminus of the cave inflow with a 315 meters depth. Figure (**2**) shows the vehicles that were used in this cave.

Nevertheless, it is honorable to mention the great records that were marked outside France. Particularly, the famous Italian cave *"Pozzo del Merro"* gained its reputation in 2000 when the two ROV *Mercurio* and *Hyball 300* reached respectively 210m and 310m depth [**5**]. Later after two years, Prometeo hit the lowest with a record breaking of cave diving of 392 meters in history of caves exploration. Indeed, this karst formation was formed by volcanic activity. It wasn't until 2016 that the legendary polish diver Krzysztof Starnawski led a Czech-polish team into the "Hranická Propast" cave, without mentioning the struggles of the team since 1999 of reaching the bottom of the cave due to the volcanic material that was not safe for the divers, where he managed to send a ROV by GRALmarine, shown in Figure (**3**), and achieved the lowest point ever recorded for an ROV in cave diving and also the deepest underwater cave of 404 meters surpassing *"Pozzo del Merro"* by 12 meters.

It can be seen from figure (**4**) that it is undeniable to conclude that diving deeper than 40 meters is 3.5 times more likely to be ended up in a deadly incident. According to *Buzzacott et al*[**7**] , the most common causes of death in cave diving exploration is greatly linked to drowning, which is usually followed by running out of air. Nevertheless, the occurrence of such miseries is due to getting lost and poor gas planning.

*Figure 2 Télénaute (left) Sorgonaute (center) Spélénaute (right) [**4**]*

Figure 3 Hranicka Propast cave, Czech Republic, cave remarkable history (left), GRALmarine ROV (right)

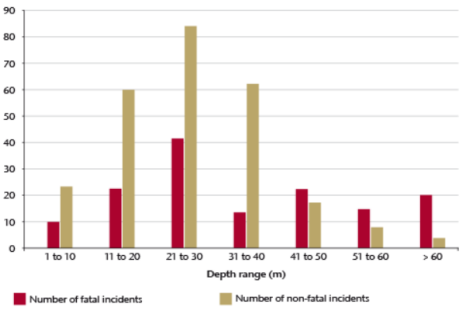

Figure 4 A comparison of the depths of fatal and non-fatal incidents [6]

Therefore, it is of upmost importance in this paper to propose a new method and design for underwater cave diving ROV that will be able to challenge most of the engineering questions and scientific difficulties for robotics for karst exploration in regards to safety and efficiency. The problem arisen here is related to the complexity of topology, variable sections and closed space environments. Additionally, although an ROV can reach the terminus of the cave, the question is still open to what ends and limits the water flow going inside the terminus could leads. The challenge this paper must face is whether it is possible to reach beyond and deeper than it is possible with the current ROV designs and methods. This question is clearly relatable to the redundancy of the robot at any given time and any given pose or orientation. Therefore, in the case of a fully redundant system whereas every degree of freedom could be achievable in more than one possibility, the problem can still remain with the battery's limitation and whether if it is possible to build a system that is able to save energy to go this much of depth. Another constraint is related to the cable length which is a real problem in underwater robotics even in open sea missions. It is still difficult to send an expensive robot autonomously without a human touch to secure a safe return for the ROV.Therefore, **this paper focus on the design and modelling and configuration of a redundant eel-like(snake) system that will be able to deal with these requirements.**

It should be noted that this paper doesn't not discredit the method and design of previous ROV but only try to proves whether an underwater eel-like system with multiple thrusters can either solve the challenges with a new technique and method for underwater karst cave exploration.

V. HADES

1. Snake locomotion

It is undisputable that most of the engineering designs has gained inspiration from mother nature while searching ideal solutions for problems. This paper will address the biomimetics of snakes, the first ever records on this subject was studied by J. Gray [7] which was the pioneer on studying snake locomotion and mathematical modelling of snake movements. It wasn't until the work of Hirose [8] when the first endeavors of developing the first snake robot succeeded but the complexity of this system was ahead of its time to control such high number of DOF.The work of Hirose was fascinating to conclude that indeed the movements of biological snakes depends on the ground friction, temperature and other external effects. The most well known and used movements biologically, shown in figure (5), are assumed to be:

- *Lateral undulation:* Most common snake locomotion with the highest speed, in this type of movement, the snake body push against irregularities in the surface which push the snake forward. Every point of the snake's body pass at the same point on the ground thus there is no static contact between any other point and the body. However, in underwater, snake locomotion is similar but instead the body push against fluid friction.
- *Concertina Locomotion:* It is usually used in confined spaces, particularly, this type of movement is conducted by pushing the front head forward while the back part is curved in a sinusoidal shape where one or more anchors are positioned against the tight environment. This type of motion is not efficient in terms of energy consumption however the design and modelling of our system should consider this movement knowing that karst caves are fully confined and complex. It is interesting to consider this movement as a constraint in our study.
- *Rectilinear crawling:* Extremely complex to imitate in a robot locomotion but it should be an honorable mention. It is used by snakes when approaching their prays to minimize their speed and prepare for a high jump. Half of the body consists of stretching while the other is pulling at the same time to push it self.
- *Sidewinding:* Similar to Concertina Locomotion, it is usually used by desert's eels, one part of the body acts as an anchor while the other is moving forward. However, in this case the heading is oriented by a 45º.This could also be used by our system's control strategy and motion planning to overcomes confined spaces while maintaining a safety for the design.

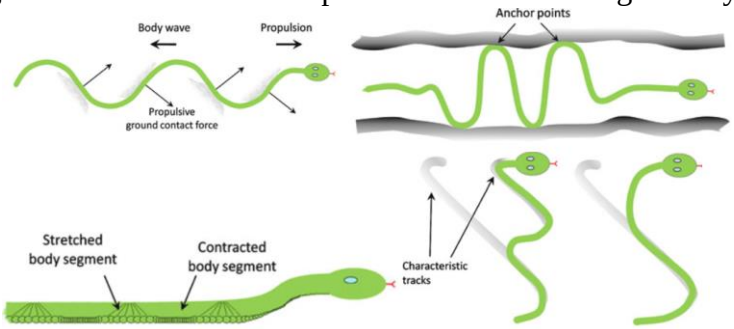

Figure 5 (Upper left)-Lateral undulation. (Upper right)-Concertina locomotion. (Lower left)-Rectilinear crawling. (Lower right)-Sidewinding. [9]

Robotics research on underwater snakes was pioneered by McIsaac and Ostrowski (2003) [**10**] which was propelled by hydrodynamics forces. However, it wasn't until Boyer et al. (2006) [**11**] and Zuo et al (2008) [**12**] that the first principles of employing a dynamic model of a swimming snake robot. The work in underwater eel like systems came handy with the remarkable work of the Norwegian laboratory NTNU with the leading researcher of Kristin Ytterstad Pettersen which was the founder of Eelume (shown in Figure **6**),2015, the only recorded existence of an underwater snake robot propelled by thrusters and snake locomotion-like movements. The work of K. Pettersen, J. Thygeson and E. Kelasidi [**13**] [**14**] [**15**] [**16**], focused on the modeling and design of an underwater snake robot that is capable of being propelled by its thrusters and also imitating the snake-like movements of Lateral undulation.

*Figure 6 Eelume design and components [**17**]*

With the Eelume being a combination of joints, thrusters and various payload modules therefore the slender body can be precisely hovered and maneuvered in any case. It can also be noticed that the head can have multiple gadget that can be introduced to carry out subsea pipeline inspection. Indeed, the Eelume dominates/will dominates the subsea in terms of inspection. Nevertheless, in this paper the question is open for karst exploration and whether an eel-like system is capable of challenging all these aspects to go deeper than any ROV achieved in the last decades.

2. Design

Lionel Lapierre, the supervisor of this paper, suggested the eel-like system to go beyond the scope of current ROVs in underwater karst caves. The answer to his question was the hybrid of Eelume and current ROVs, however such system is complex to build, design, control, maneuver and the robotics solution could still be difficult and not to mention the batteries capabilities of maintaining such system. This paper will address these issues by introducing **Hades**, the robot was designed by Solidworks, a 3D modelling Computer Aided Design. Optimally, our design considered the following constraints:

- Although existing snake robots without thrusters or only surge direction thrusters are able to be fully redundant when having some reconfigurable shapes. The design of **Hades** shall address this issue by having a fully redundant system without having to reconfigure the shape of the robot. In other words, the robot should be able to have ***6 DOF at any given time*** independently of the joint's configuration.

- By pointing out the above point, it should also be noted that a joint system shall be designed in a way that **Hades** shall be able to manipulate and orientate in the yaw and pitch. Indeed, the roll here is not included for an obvious reason which is useless to orientate a fully symmetric robot around the YZ plane and having a roll (rotation around the X-axis), the resulting configuration will end up in a similar shape. Another reason is the resulting forces could change and end up in a very complex scene where the robot will not be able to counteract all the resulting torques. To minimize this issue, the design will stick to maintain only a ***yaw and pitch orientations***. Thus, assuming the snake is divided to multiple sections cylinders, each section shall be separated by a 2 DOF joints that can rotate in the yaw and pitch orientations.
- As it was mentioned before and in most robotics designs, symmetry is an optimal pursuit to have a system that is not complex by its own nature. Convincingly, the snake shape is similar to a submarine or ellipsoid where it is symmetrical to all its axis. However, this would be true ofcourse when the joints are in a state where each joints have different angle orientation. Therefore, the robot must be ***symmetrical*** when the joints configuration is at its initial states.
- In order to have 6 DOF, symmetrical and 2 DOF joints. The thruster's configuration should be situated in a manner where there is 1 thruster on each side of the cylinders in a way where the final resulting direction for each axis has 4 thrusters totally thus 12(3x4) thrusters in total, and two coupled thrusters on any side. This can be seen ofcourse in the 3D CAD and it is illustrated much more clearly.
- The batteries should be confronted in the design where each cylinder shall be able to host battery cells connected by each other in an inner section. The design in this paper will not go deeply how the wires are distrusted. This shall be investigated later when the mechanical part is focused on separately to have a safe design.
- The last major constraints should focus on the smoothness of the snake and how the head snake design shall be designed in an efficient way and least energy consuming to guarantee the best optimal speed for the least amount of energy loss (this part will be studied in this paper in the CFD section to ensure that the design is realistic)

The design is shown in figure (**7**), (**8**), (**9**) and (**10**) where it can be seen that the eel-like robot is almost perfectly symmetrical. Notice how the 2 DOF servomotors are placed perpendicularly so the yaw and pitch orientation can be controlled. It should be noted that the thrusters are chosen to be the T-200 of the blue robotics which has around a 65 Newton of full thrust. **Hades** can also work as a robotics hands underwater that is maneuverable as an ROV system. This gives **Hades** the title of being the only dual-robotics arms that can be operated underwater while being controlled by its thrusters. For sure such assumption would need time to be proven with more advancing studies. The other configuration systems are multiple and will be explained later in following section to investigate the configuration matrix for different pose.

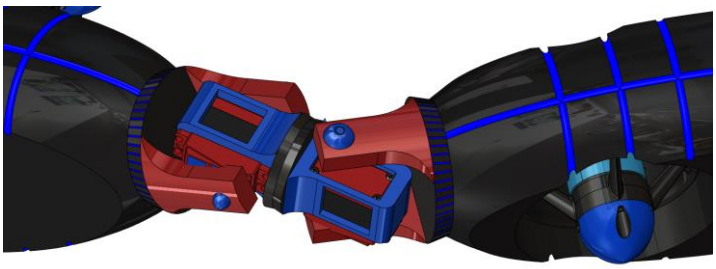

Figure 7 Hades, joints 2 DOF view skeleton

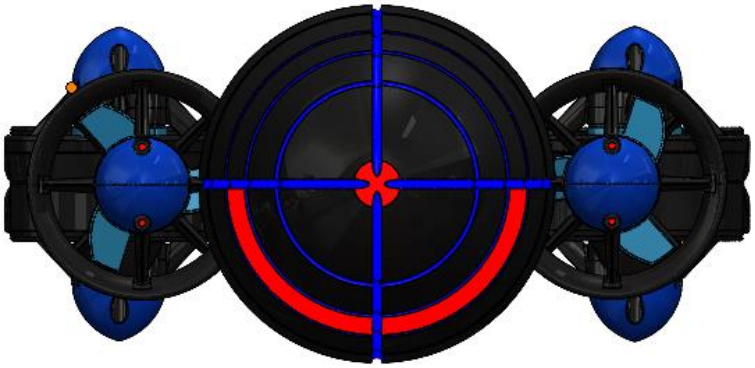

Figure 8 Hades' front view

Figure 9 Hades' upper view

Figure 10 Hades, the fully redundant system with grippers and explorer of the underworld

3. Computation Fluid Mechanics

This section investigates the dynamics mechanically in order to prove whether such system is realistic to implement and whether the design is fully optimized. Indeed, the study of drag and turbulence along the fluid flow around the body can only be calculated by CFD analysis accurately to ensure that the robotic system does not suffer from stability issues which is one of the most threatening topics when it comes to the study of aerodynamical and hydrodynamical vehicles. Additionally, this section can also confirm whether our system is symmetrical enough which depends ofcourse on the multiple forces that are varying on the other axis of the fluid flow. The analysis was made using ANSYS fluent software which is dedicated for CFD analysis

The paper will not explain how CFD works or the procedure since it is another big domain that is not the main issue, therefore, the paper will go straight to the results. After obtaining a mesh as shown in Figure **11**, and it can be illustrated that the model is being simulated in a wind tunnel where the fluid is attacking the ROV from the Surge direction.

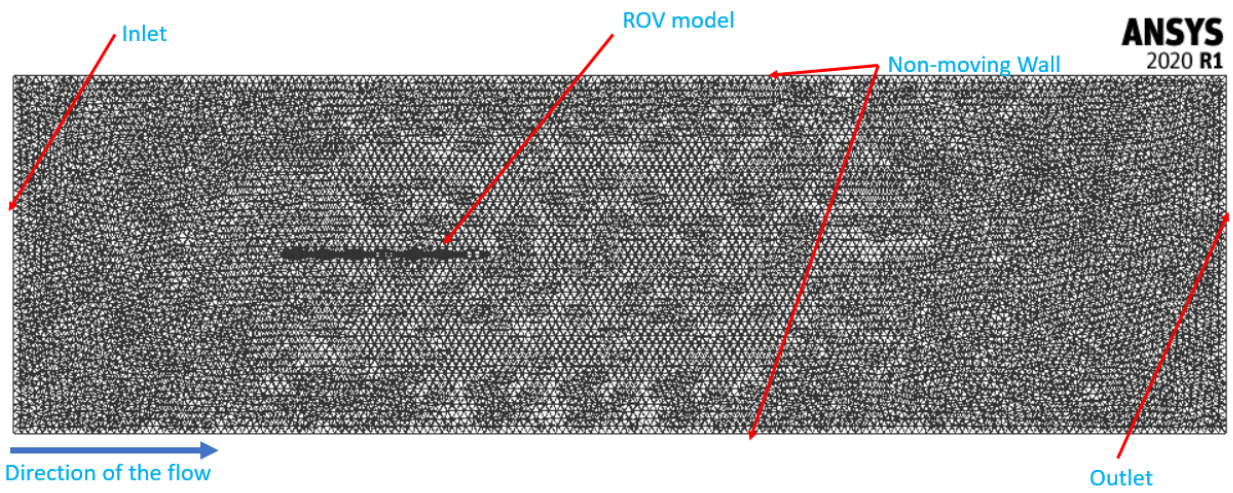

Figure 11 3D mesh of the ROV model for simulation

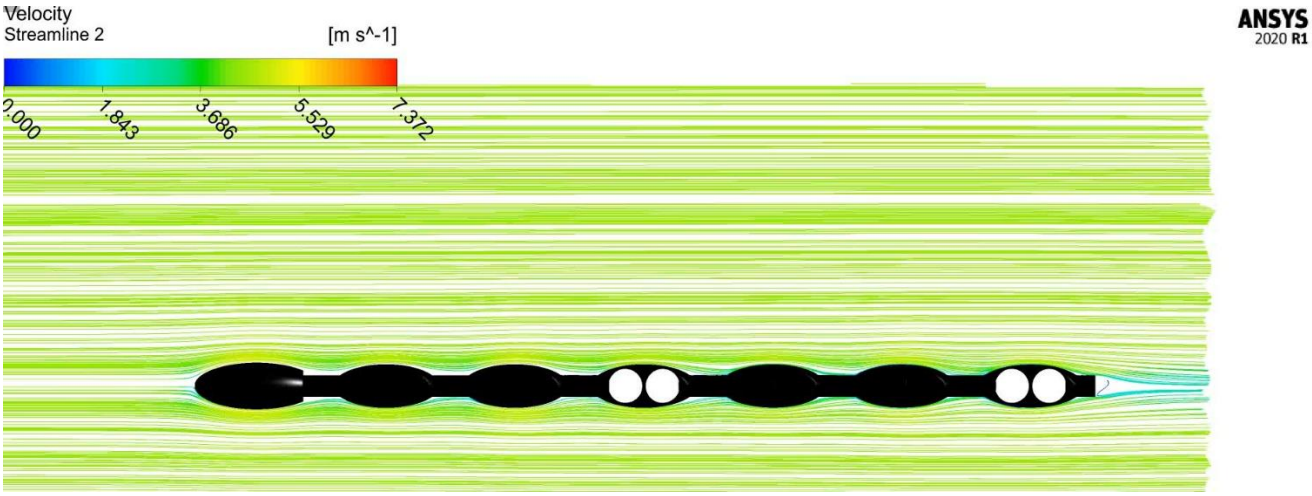

Figure 12 CFD results, Fluid velocity streamlines along the x direction (left to right flow direction)

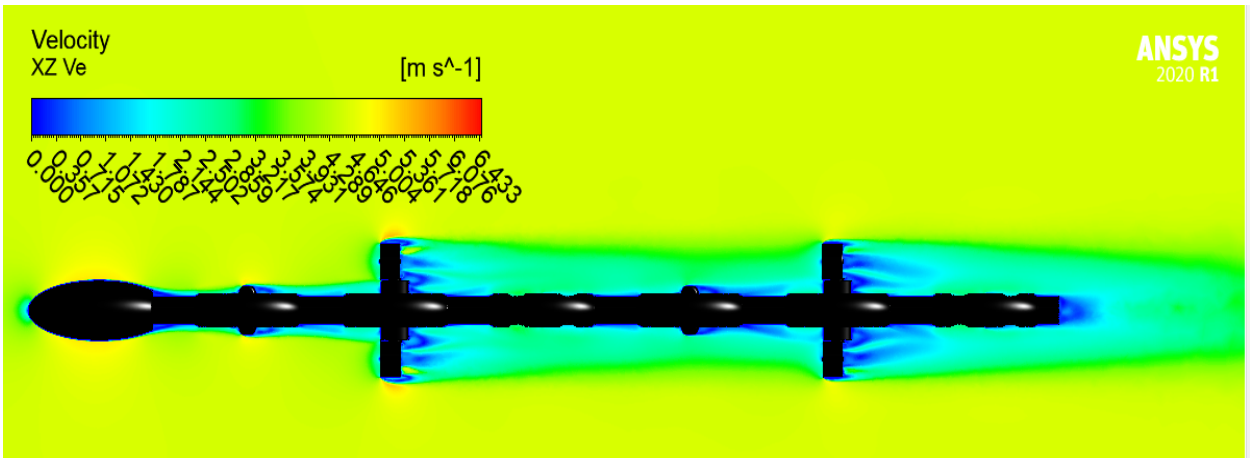

Figure 13 CFD results, Velocity contour of the fluid flow (left to right flow direction)

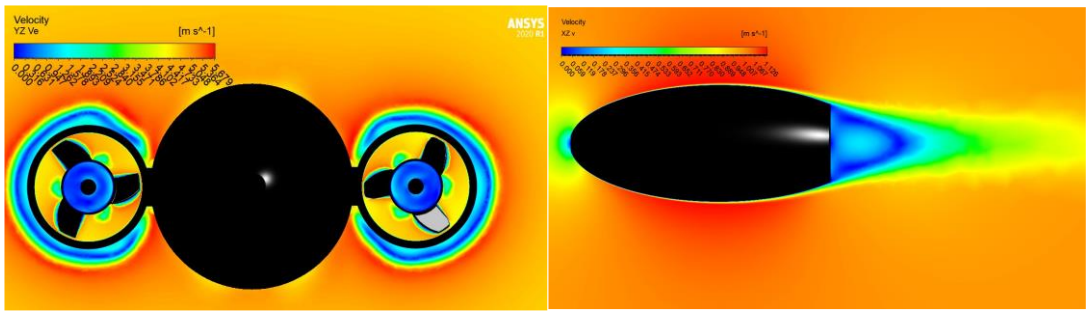

Figure 14 velocity contour along the thrusters(left), velocity contour of the snake head(right)

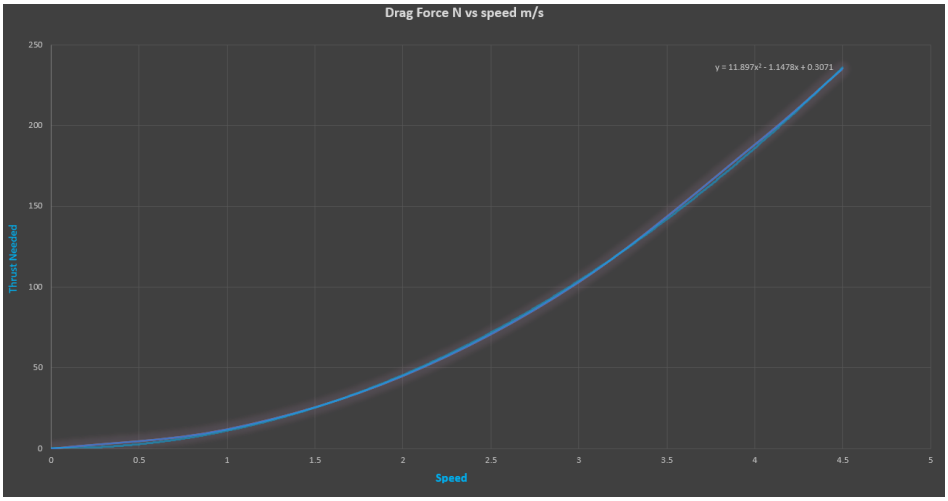

Figure 15 Thrust needed for the motor's vs ROV speed

It should be noted, around 8 simulations (72 hours each averagely) were made to obtain the graph of figure (**15**). Each simulation calculated the thrust that is needed in order for the ROV to have the desired speed. After each simulation, Data was collected and the graph was finally plotted in order to get the least squared second-degree plot of this graph. From the Figure (**12**), the CFD results can confirm that the streamline on our snake is smooth and does not suffer from turbulence, indeed to confirm this, the observer has to look at the end of the model and note how the streamlines on the outlet is almost parallel to the streamline on the inlet. This can confirm that the turbulence is low and thus the stability is safe to assume. On Figure (**13**), the velocity contours shows that there is some significant turbulence (in red) on the surge thrusters which is normal in terms of hydrodynamics, but what it is interesting is that the thrusters' turbulence does not depends on the fronts. In other words, the model is stable and the 4 thrusters that represent the surge direction has almost no correlation and dependency. Indeed, this prove a key point in the design's success. Figure (**14, left**), can confirm the previous statement whereas figure (**14, right**), shows that the snake head design is a perfect shape where the velocity is 0 on the center line and it is maximum on the biggest radius of this ellipsoid. As it was mentioned before, the snake head has the biggest effect on the turbulence and stability of the whole ROV.It should also be noted that the forces on Y and Z axis are almost null which is an outstanding result given that the drone will not have not have any uncontrollable maneuvers when moving just on the X axis. This CFD section is key to prove that the design is successfully in terms of dynamics and stability and that **Hades** can be safely assumed as a potential underwater's fastest ROV given that 4.5 m/s as a result is a much more above than the average in terms of ROV speed.

4. Lagrangian differentiation

Generally, Euler-Newton equations are straightly used in underwater robotics to build the kinematical model (equation can be seen in the following page). However, in the case of Hades, the Euler-Lagrange should be chosen without a second thought, since the robot has multiple thrusters that depends on 14 servomotors at least therefore a deformable system with more than a million configuration. This can be only simply modelled by Euler-Lagrange [**18**] [**19**] [**20**] which dominates other methods. On the other side, not many literature deals with underwater snakes' system since most of the literature is still concerned about surface eel-like systems. Therefore, some of the equations concerning the added mass, added Coriolis and hydrodynamical equations will not be derived since it can be used in any underwater system therefore these matrices will be used from the general equations that was developed by Fossen [**21**] and they are shown in appendix (**C**). However, this paper will develop the kinematics concerning the joints and thrusters which are the main purpose here. From figure **16**, **17** and **18** in appendix **A** we denote θ_n and φ_n as the pitch and yaw angles respectively in reference to the inertial frame. N refers to the numbers of links(cylinders) where N-1 joints exists.$[x_h, y_h, z_h]$ are the position of the frontal head and l represents the length from the center of the link to one of the extremities. The angles are considering not relatives therefore θ_n does not includes θ_{n-1} (considering it known to reduce variables). Therefore, the space vector considered here is.$q_n = [x_h, y_h, z_h, \theta_1, \varphi_1, \dots, \theta_n, \varphi_n]$.The differentiation will be shown in appendix (**B**) but let's start by:

$$x_n = x_h + 2l + \sum_{i=2}^{N-1} 2l \cos\theta_i \cos\varphi_i + l\cos\theta_n \cos\varphi_n$$

$$y_n = y_h + \sum_{i=2}^{N-1} 2l \sin\varphi_i + l\sin\varphi_n$$

$$z_n = z_h + \sum_{i=2}^{N-1} 2l \sin\theta_i + l\sin\theta_n$$

After differentiation each of $[x_n, y_n, z_n]$, the velocity equations will be put in Lagrange equation given by:

$$\frac{\partial}{\partial t}\left(\frac{dT}{d\dot{q}}\right) - \left(\frac{dT}{dq}\right) + \left(\frac{dR}{d\dot{q}}\right) = AF$$

Where T represents the kinetic energy, R represents the potential (V derived in the appendix) and hydrodynamical equation (will used Fossen equation straight out). AF represents the output forces; they will be explained briefly in the next section.

The results of the derivation will match the equations of Euler-Newton which is shown in appendix. However, the real profit is the method used with Lagrange where the variable of each state can be calculated. As an example, it is possible now to calculate the forces on joints 7th that is somehow being varied by the rotation of the 1st joint. In the appendix, the derivation was made solely on the first 3 joints. However, a MATLAB code was made to calculate the equation of the whole system *symbolically* and then alter transformed into matrices.

5. Configuration matrix

From Fossen [22] the fully developed equation for hydrodynamics in the Euler-Newton approach is given by (shown in appendix *C*):

$$\mathrm{M_{RB}}\dot{\mathrm{v}} + \mathrm{C_{RB}}(\mathrm{v})\mathrm{v} + \mathrm{M_A}\dot{\mathrm{v}} + \mathrm{C_A}(\mathrm{v})\mathrm{v} + \mathrm{D}(\mathrm{v})\dot{\mathrm{v}} + \mathrm{g}(\eta) + \mathrm{g_0} = \mathrm{F}_B + \tau_{\mathrm{wind}} + \tau_{\mathrm{wave}}$$

$$Rigid-body\ forces \begin{cases} M_{RB}\ mass\ matrix \\ C_{RB}\ coriolis\ matrix \end{cases}$$

$$Hydrodynamic\ forces \begin{cases} M_A\ which\ represents\ the\ added\ mass\ matrix \\ C_A\ which\ represents\ the\ coriolis-centripetal\ added\ mass\ matrix \\ D\ which\ represents\ the\ Damping\ matrix(can\ be\ calculated\ by\ CFD) \end{cases}$$

$$Hydrostatics\ forces \begin{cases} g(\eta)\ which\ represents\ the\ gravitation, buoyancy\ forces\ and\ moments\ vector \\ g_0\ which\ represents\ the\ ballast\ control\ forces\ vector \end{cases}$$

$$Output\ forces \begin{cases} \tau\ \ which\ represents\ the\ thrust\ output\ forces \\ \tau_{wind}\ which\ represents\ the\ wind\ forces \\ \tau_{wave}\ which\ represents\ the\ wave\ induced\ forces \end{cases}$$

In this paper we will focus on A which is the configuration matrix and it should be found when calculating the resulting output forces given by:

$$\mathrm{F}_B = \mathrm{A}.\,\mathrm{F}_m = \begin{pmatrix} F \\ \tau \end{pmatrix}$$

However, the complexity of this system suffers from the numbers of thrusters (12) which also depends on the 14 joints in the design, therefore and although a mathematical approach was tried in the Euler-Newton, it can be seen in the appendix **D** how this approach is beyond the scope of manually *deriving it*. A MATLAB code was then developed to calculate the configuration matrix A depending on every joint's orientation. Therefore, the purpose is to calculate the redundancy of every major configuration that **Hades** will be put out in order to confirms whether such system is 6 DOF.

In fact, $\mathrm{F}_B = [\mathrm{F}_u, \mathrm{F}_v, \mathrm{F}_w, \tau_p, \tau_q, \tau_r] \in \mathbb{R}^6$ is the resulting vector which corresponds to the resulting forces and torques. $\mathrm{F}_B = \left[\mathrm{F}_{t,1}, \mathrm{F}_{t,2}, \mathrm{F}_{t,3}, \dots, \mathrm{F}_{t,n}\right] \in \mathbb{R}^t$ where *t* is related to the number of thrusters.

Matrix A can be rewritten as:

$$A = \begin{pmatrix} u_1 & u_2 & \dots & u_t \\ d_1 r_1 \otimes u_1 & d_2 r_2 \otimes u_2 & \dots & d_t r_t \otimes u_t \end{pmatrix}$$

$d_t r_t$ represents the direction times the length between the thruster and the center of the body-frame.

The major condition for an ideal system is to have the *rank(**A**)=6* in order to have a fully deformable, redundant, full actuated system. Despite that, having rank(A)==6 does not qualify the ROV to have 6 DOF, the reason could be that some forces would adds up to give 0 forces in the end. therefore, F_B should also be taken into account.

In order to prevent very low values that could still make rank(A)==6. The following algorithm will be made where:

$$\sum_{i}^{t} \|u_i\|^2 \ \ for\ each\ row$$

$$\sum_{i}^{t} \|\tau_i\|^2 \ \ for\ each\ row$$

u_i, τ_i,are the coefficients of the matrix A. once A is summed and squared, an algorithm will be implemented to check whether low values exists so they can be neglected while calculating *rank(A)*

In any case, the study will be on general form that Hades could be deformed into and the MATLAB code will calculate and show whether such configuration is fully actuated. Starting by the U shape, the MATLAB figure is shown in figure **19**, where this kind of configuration could be used when the robot is scanning a karst that has a U turn, another application could be while using both grippers to transport anything along. From the results it can be seen that the rank is 5 which is understandable and on purpose to show that the snake is not always fully actuated but also under actuated in some cases.

By deforming into a O shape, shown in figure **20**, this configuration could be used for doing a rotation around the snake or also trying to manipulate an object under water, the results shows that the rank is 6 indeed. Notice how the torque coefficients are relatively low compared to the forces which is needed in order to control the stability in a much smoother way.

The L shape is shown in figure **21**, this movement is key and needed for entering karst that has different kind of inlet direction than the outlet, therefore it is important to deform the snake.the rank of this configuration shows to be 5 , however notice how the 4^{th} row is not completely zero, however the algorithm is structured to remove low numbers for its insignificant effect on the actuation.

The gamma and S shapes can be both shown in figure 22 and 23, this kind of configuration are used for concertina locomotion which was explained previously, notice how the ranks are not 6 even though their rows are not null. This kind of maneuverings becomes complex and the robot orientation is only temporally in these configurations in order for the snake to reset its self when it is no longer in a confined environment.

Some random shapes were made in order to show how complex the snake control and how much solution exists for every type of configuration. This type of configuration should be avoided in case unless the robot is susceptible to any kind of potential damage where this kind of configuration is needed to for wall avoidance.

Nevertheless, it can be shown how the ranks varies in different kind of configuration depending on the orientation of 14 servomotors.

VI. Conclusion

In this paper, we have introduced **Hades**, a potential underwater snake robot that could dominate the underworld. The main purpose is to explore the complex Karst geographical systems that will enable the researchers of the future era to be more aware of a potential hazardous flooding, also the study of this system will enable researchers to have better study on the water pollution and nutrient cycles in engineering geosciences and agriculture geology.

Several studies were made by ANSYS for CFD analysis to prove that **Hades** has the rightful claim to dominate these quests and operations. The design of Hades proved to have a promising potential with a no stability issues or turbulences which also comes with a high speed for underwater ROV.

Then again, mathematical modelling and kinematics with Lagrangian formulation were derived in order find whether it is possible to make this system controllable with all its complex features. The answer came with the Thruster configuration matrices for every shape, the robot proved that it deforms in any shape and still have the possibility to orientate and position in any dimension, ofcourse depending on its joint's orientations. However, some concerns can be risen whether **Hades's** future control system can avoid cases where the robot is under actuated. Ofcourse as it was shown, the robot is underactuated in some cases but given its locomotion, the robot can deform and change its odds thanks to its 14 servomotors.

Future work, this paper is an introduction for an engineering challenge that has many open doors, the question is not whether this system will be implemented or not in the future. The question should be when such system will reach the underworld? **Eelume** has the potential claim to be dominating the underwater robotics and it is already a successful engineering system for pipeline inspections. However, **Hades** 'additional features and degrees of freedom can challenge the world's most innovative robot and not forgetting that Karst exploration remains intact of having a snake robot mission.

Finally, I would like to thank Professor. Lionel Lapierre for supervising me for this project. I have gained much knowledge under his hands. This was a great introduction for me for greater things and many thanks to him since most of the motivation and inspiration stayed on hype because of him. I expected to deal and reach the dynamics control part where I could have the possibility to simulate such robot but for sure this type of project needs years of studies and timeless research to have a god in our underworld but *as a wise person once said: "Good things takes time"*

VII. Appendix

A. Mathematical representation of the snake

Heave plane x-y , rotation Yaw

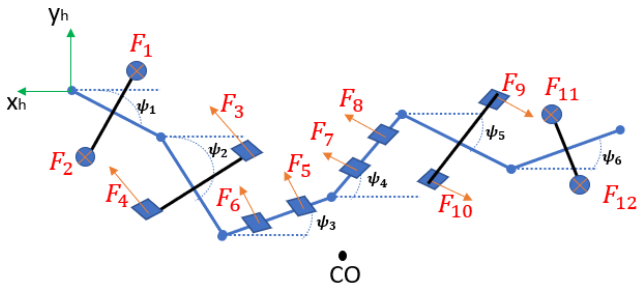

Figure 16 Mathematical representation of the snake, heave plane

Sway plane x-z rotation pitch

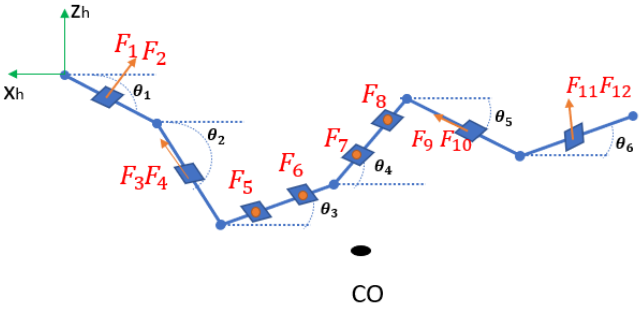

Figure 17 Mathematical representation of the snake, Sway plane

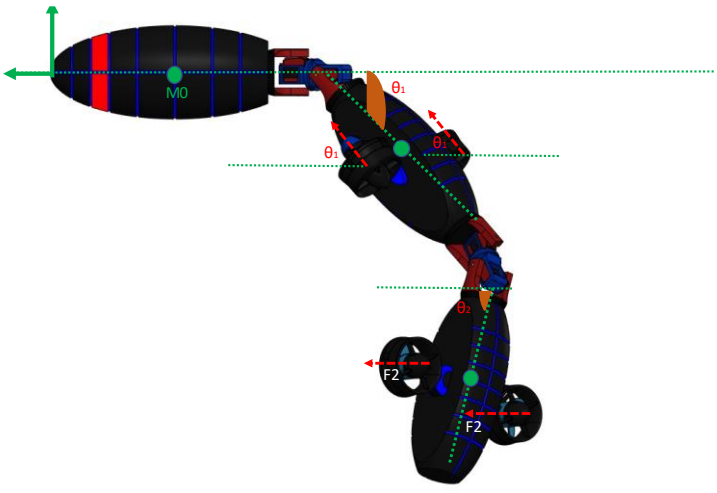

Figure 18 3D representation of the kinematical model

B. Derivation

$$x_0 = x_h + l$$

$$x_1 = x_h + 2l + l\cos\theta_1\cos\varphi_1$$

$$x_2 = x_h + 2l + 2l\cos\theta_1\cos\varphi_1 + l\cos\theta_2\cos\varphi_2$$

…..

$$x_n = x_h + 2l + \sum_{i=2}^{N-1} 2l\cos\theta_i\cos\varphi_i + l\cos\theta_n\cos\varphi_n$$

$$y_0 = y_h$$

$$y_1 = y_h + l\sin\varphi_1$$

$$y_2 = y_h + 2l\sin\varphi_1 + l\sin\varphi_2$$

…..

$$y_n = y_h + \sum_{i=2}^{N-1} 2l\sin\varphi_i + l\sin\varphi_n$$

$$z_0 = z_h$$

$$z_1 = z_h + l\sin\theta_1$$

$$z_2 = z_h + 2l\sin\theta_1 + l\sin\theta_2$$

…..

$$z_n = z_h + \sum_{i=2}^{N-1} 2l\sin\theta_i + l\sin\theta_n$$

Velocities:

$x_0 = x_h + l \rightarrow \dot{x_0} = \dot{x_h}$

$x_1 = x_h + 2l + l\cos\theta_1\cos\varphi_1 \rightarrow \dot{x_1} = \dot{x_h} - l\left(\dot{\theta_1}\sin\theta_1\cos\varphi_1 + \dot{\varphi_1}\cos\theta_1\sin\varphi_1\right)$

$x_2 = x_h + 2l + 2l\cos\theta_1\cos\varphi_1 + l\cos\theta_2\cos\varphi_2$

$\rightarrow \dot{x_2} = \dot{x_h} - 2l\left(\dot{\theta_1}\sin\theta_1\cos\varphi_1 + \dot{\varphi_1}\cos\theta_1\sin\varphi_1\right) - l\left(\dot{\theta_2}\sin\theta_2\cos\varphi_2 + \dot{\varphi_2}\cos\theta_2\sin\varphi_2\right)$

…..

$\rightarrow \dot{x_n} = \dot{x_h} + \sum_{i=2}^{N-1} -2l\left(\dot{\theta_i}\sin\theta_i\cos\varphi_i + \dot{\varphi_i}\cos\theta_i\sin\varphi_i\right) \quad - l\left(\dot{\theta_n}\sin\theta_n\cos\varphi_n + \dot{\varphi_n}\cos\theta_n\sin\varphi_n\right)$

$y_0 = y_h \rightarrow \dot{y_0} = \dot{y_h}$

$y_1 = y_h + l\sin\varphi_1 \rightarrow \dot{y_1} = \dot{y_h} + l\dot{\varphi_1}\cos\varphi_1$

$y_2 = y_h + 2l\sin\varphi_1 + l\sin\varphi_2 \rightarrow \dot{y_2} = \dot{y_h} + 2l\dot{\varphi_1}\cos\varphi_1 + l\dot{\varphi_2}\cos\varphi_2$

…....

➔ $\dot{y_n} = \dot{y_h} + \sum_{i=2}^{N-1} 2l\dot{\varphi_i} \cos\varphi_i + l\dot{\varphi_n} \cos\varphi_n$

$z_0 = z_h$➔$\dot{z_0} = \dot{z_h}$

$z_1 = z_h + l \sin\theta_1$➔$\dot{z_1} = \dot{z_h} + l\dot{\theta_1} \cos\theta_1$

$z_2 = z_h + 2l \sin\theta_1 + l \sin\theta_2$➔ $\dot{z_2} = \dot{z_h} + 2l\dot{\theta_1} \cos\theta_1 + l\dot{\theta_2} \cos\theta_2$

…….

➔ $\dot{z_n} = \dot{z_h} + \sum_{i=2}^{N-1} 2l\dot{\theta_i} \sin\theta_i + l\dot{\theta_n} \sin\theta_n$

Accelerations:

$\ddot{x_0} = \ddot{x_h}$

$\dot{\ddot{x_1}} = \ddot{x_h} - l\left(\dot{\theta_1} \sin\theta_1 \cos\varphi_1 + \dot{\varphi_1} \cos\theta_1 \sin\varphi_1\right)$

$= \ddot{x_h} - l\left(\ddot{\theta_1} \sin\theta_1 \cos\varphi_1 + \dot{\theta_1}^2 \cos\theta_1 \cos\varphi_1 - \dot{\theta_1}\dot{\varphi_1} \sin\theta_1 \sin\varphi_1 + \ddot{\varphi_1} \cos\theta_1 \sin\varphi_1 + \ddot{\varphi_1}^2 \cos\theta_1 \cos\varphi_1 - \dot{\theta_1}\dot{\varphi_1} \sin\theta_1 \sin\varphi_1\right)$

$\ddot{x_2} = \ddot{x_h} - 2l\left(\ddot{\theta_1} \sin\theta_1 \cos\varphi_1 + \dot{\theta_1}^2 \cos\theta_1 \cos\varphi_1 - \dot{\theta_1}\dot{\varphi_1} \sin\theta_1 \sin\varphi_1 + \ddot{\varphi_1} \cos\theta_1 \sin\varphi_1 + \ddot{\varphi_1}^2 \cos\theta_1 \cos\varphi_1 - \dot{\theta_1}\dot{\varphi_1} \sin\theta_1 \sin\varphi_1\right) - l\left(\ddot{\theta_2} \sin\theta_2 \cos\varphi_2 + \dot{\theta_2}^2 \cos\theta_2 \cos\varphi_2 - \dot{\theta_2}\dot{\varphi_2} \sin\theta_2 \sin\varphi_2 + \ddot{\varphi_2} \cos\theta_2 \sin\varphi_2 + \ddot{\varphi_2}^2 \cos\theta_2 \cos\varphi_2 - \dot{\theta_2}\dot{\varphi_2} \sin\theta_2 \sin\varphi_2\right)$

….

➔

$\ddot{x_n} = \ddot{x_h} + \sum_{i=2}^{N-1} -2l\left(\ddot{\theta_i} \sin\theta_i \cos\varphi_i + \dot{\theta_i}^2 \cos\theta_i \cos\varphi_i - \dot{\theta_i}\dot{\varphi_i} \sin\theta_i \sin\varphi_i + \ddot{\varphi_i} \cos\theta_i \sin\varphi_i + \ddot{\varphi_i}^2 \cos\theta_i \cos\varphi_i - \dot{\theta_1}\dot{\varphi_i} \sin\theta_i \sin\varphi_i\right) - l\left(\ddot{\theta_n} \sin\theta_n \cos\varphi_n + \dot{\theta_n}^2 \cos\theta_n \cos\varphi_n - \dot{\theta_2}\dot{\varphi_n} \sin\theta_n \sin\varphi_n + \ddot{\varphi_n} \cos\theta_n \sin\varphi_n + \ddot{\varphi_n}^2 \cos\theta_n \cos\varphi_n - \dot{\theta_n}\dot{\varphi_n} \sin\theta_n \sin\varphi_n\right)$

$\ddot{y_0} = \ddot{y_h}$

$\ddot{y_1} = \ddot{y_h} + l\ddot{\varphi_1} \cos\varphi_1 - l\dot{\varphi_1}^2 \sin\varphi_1$

$\ddot{y_2} = \ddot{y_h} + 2l(\ddot{\varphi_1} \cos\varphi_1 - \dot{\varphi_1}^2 \sin\varphi_1) + l\left(\ddot{\varphi_2} \cos\varphi_2 - l\dot{\varphi_2}^2 \sin\varphi_2\right)$

…....

➔ $\ddot{y_n} = \ddot{y_h} + \sum_{i=2}^{N-1} 2l\ddot{(}\varphi_i \cos\varphi_i - \dot{\varphi_i}^2 \sin\varphi_i) + l\left(\ddot{\varphi_n} \cos\varphi_n - \dot{\varphi_n}^2 \sin\varphi_n\right)$

$\ddot{z_0} = \ddot{z_h}$

$\ddot{z_1} = \ddot{z_h} + l\ddot{\theta_1} \cos\theta_1 - l\dot{\theta_1}^2 \sin\theta_1$

$\ddot{z_2} = \ddot{z_h} + 2l(\ddot{\theta_1} \cos\theta_1 - \dot{\theta_1}^2 \sin\theta_1) + l(\ddot{\theta_2} \cos\theta_2 - \dot{\theta_2}^2 \sin\theta_2)$

…....

➔ $\ddot{z_n} = \ddot{z_h} + \sum_{i=2}^{N-1} 2l\ddot{(}\theta_i \cos\theta_i - \dot{\theta_i}^2 \sin\theta_i) + l\left(\ddot{\theta_n} \cos\theta_n - \dot{\theta_n}^2 \sin\theta_n\right)$

Euler-Lagrange Equation:

$$\frac{\partial}{\partial t}\left(\frac{dT}{d\dot{q}}\right)-\left(\frac{dT}{dq}\right)+\left(\frac{dR}{d\dot{q}}\right)=AF+J$$

$T=\frac{1}{2}m\dot{x}_1^2+\frac{1}{2}m\dot{x}_0^2+\frac{1}{2}m\dot{y}_1^2+\frac{1}{2}m\dot{y}_0^2+\frac{1}{2}m\dot{z}_1^2+\frac{1}{2}m\dot{z}_0^2+\frac{1}{2}J\dot{\theta}_1^2+\frac{1}{2}J\dot{\varphi}_1^2$

$$T=\frac{1}{2}m\left(\dot{x_h}-l\left(\dot{\theta}_1\sin\theta_1\cos\varphi_1+\dot{\varphi}_1\cos\theta_1\sin\varphi_1\right)\right)^2+\frac{1}{2}m(\dot{x_h})^2+\frac{1}{2}m(\dot{y_h}+l\dot{\varphi}_1\cos\varphi_1)^2+\frac{1}{2}m(\dot{y_h})^2+\frac{1}{2}m\left(\dot{z_h}+l\dot{\theta}_1\cos\theta_1\right)^2+\frac{1}{2}m(\dot{z_h})^2+\frac{1}{2}J\dot{\theta}_1^2+\frac{1}{2}J\dot{\varphi}_1^2$$

$$V=\sum_{i=1}^{n}m_igz_i=\left(\sum_{j=1}^{n}\left\{\left(m_j-\rho V_j\right)g\left[z_h+\sum_{i=1}^{j-1}2l\sin\theta_i+l\sin\theta_j\right]\right\}\right)$$

$$\left(\frac{dT}{d\dot{x_h}}\right)=m\left(\dot{x_h}-l\left(\dot{\theta}_1\sin\theta_1\cos\varphi_1+\dot{\varphi}_1\cos\theta_1\sin\varphi_1\right)\right)+m\dot{x_h}$$

$$=2m\dot{x_h}-ml\left(\dot{\theta}_1\sin\theta_1\cos\varphi_1\right)-ml(\dot{\varphi}_1\cos\theta_1\sin\varphi_1)$$

- $\frac{\partial}{\partial t}\left(\frac{dT}{d\dot{x_h}}\right)=2m\ddot{x_h}-ml\left(\ddot{\theta}_1\sin\theta_1\cos\varphi_1+{\dot{\theta}_1}^2\cos\theta_1\cos\varphi_1-\dot{\theta}_1\dot{\varphi}_1\sin\theta_1\sin\varphi_1\right)-ml\left(\ddot{\varphi}_1\cos\theta_1\sin\varphi_1+{\dot{\varphi}_1}^2\cos\theta_1\cos\varphi_1-\dot{\theta}_1\dot{\varphi}_1\sin\theta_1\sin\varphi_1\right)$
- $\left(\frac{dT}{dx_h}\right)=0$
- $\left(\frac{dV}{dx_h}\right)=0$

$$\left(\frac{dT}{d\dot{y_h}}\right)=m(\dot{y_h}+l\dot{\varphi}_1\cos\varphi_1)+m\dot{y_h}=2m\dot{y_h}+ml\dot{\varphi}_1\cos\varphi_1$$

- $\frac{\partial}{\partial t}\left(\frac{dT}{d\dot{y_h}}\right)=2m\ddot{y_h}+ml\ddot{\varphi}_1\cos\varphi_1-ml{\dot{\varphi}_1}^2\sin\varphi_1$
- $\left(\frac{dT}{dy_h}\right)=0$
- $\left(\frac{dV}{dy_h}\right)=0$

$$\left(\frac{dT}{d\dot{z_h}}\right)=m\left(\dot{z_h}+l\dot{\theta}_1\cos\theta_1\right)+m\dot{z_h}=2m\dot{z_h}+l\dot{\theta}_1\cos\theta_1$$

- $\frac{\partial}{\partial t}\left(\frac{dT}{d\dot{z_h}}\right)=2m\ddot{z_h}+ml\ddot{\theta_1}\cos\theta_1-ml{\dot{\theta}_1}^2\sin\theta_1$
- $\left(\frac{dT}{dz_h}\right)=0$
- $\left(\frac{dV}{dz_h}\right)=(m_0-\rho v_0)g+(m_1-\rho v_1)g$

$$\left(\frac{dT}{d\dot{\theta}_1}\right) = -ml\sin\theta_1\cos\varphi_1\left(\dot{x_h} - l\left(\dot{\theta}_1\sin\theta_1\cos\varphi_1 + \dot{\varphi}_1\cos\theta_1\sin\varphi_1\right)\right)$$
$$+ m\left(\dot{z_h} + l\dot{\theta}_1\cos\theta_1\right)(l\cos\theta_1) + J\dot{\theta}_1$$
$$= -ml\dot{x_h}\sin\theta_1\cos\varphi_1$$
$$+ ml^2\left(\dot{\theta}_1\sin\theta_1\cos\varphi_1\sin\theta_1\cos\varphi_1 + \dot{\varphi}_1\cos\theta_1\sin\varphi_1\sin\theta_1\cos\varphi_1\right)$$
$$+ m\dot{z_h}l\cos\theta_1 + ml^2\dot{\theta}_1\cos\theta_1\cos\theta_1 + J\dot{\theta}_1$$

- $\frac{\partial}{\partial t}\left(\frac{dT}{d\dot{\theta}_1}\right) = -ml\ddot{x_h}\sin\theta_1\cos\varphi_1 - ml\dot{x_h}\left(\dot{\theta}_1\cos\theta_1\cos\varphi_1 - \dot{\varphi}_1\sin\theta_1\sin\varphi_1\right) +$
$ml^2\left(\ddot{\theta}_1\sin\theta_1\cos\varphi_1\sin\theta_1\cos\varphi_1 + 2{\dot{\theta}_1}^2\cos\theta_1\cos\varphi_1\sin\theta_1\cos\varphi_1 -\right.$
$2\dot{\theta}_1\dot{\varphi}_1\sin\theta_1\sin\varphi_1\sin\theta_1\cos\varphi_1 - \dot{\theta}_1\dot{\varphi}_1\sin\theta_1\sin\varphi_1\sin\theta_1\cos\varphi_1 +$
$\dot{\theta}_1\dot{\varphi}_1\cos\theta_1\sin\varphi_1\cos\theta_1\cos\varphi_1 - {\dot{\varphi}_1}^2\cos\theta_1\sin\varphi_1\sin\theta_1\sin\varphi_1 +$
$\left.{\dot{\varphi}_1}^2\cos\theta_1\sin\theta_1\cos\varphi_1\cos\varphi_1 + \ddot{\varphi}_1\cos\theta_1\sin\varphi_1\sin\theta_1\cos\varphi_1\right) + m\ddot{z_h}l\cos\theta_1 -$
$m\dot{z_h}\dot{\theta}_1 l\sin\theta_1 + ml^2\ddot{\theta}_1\cos\theta_1\cos\theta_1 - 2ml^2{\dot{\theta}_1}^2\cos\theta_1\sin\theta_1 + J\ddot{\theta}_1$
- $\left(\frac{dT}{d\theta_1}\right) = -ml\left(\dot{x_h} - l\left(\dot{\theta}_1\sin\theta_1\cos\varphi_1 + \dot{\varphi}_1\cos\theta_1\sin\varphi_1\right)\right)\left(\dot{\theta}_1\cos\theta_1\cos\varphi_1 -\right.$
$\left.\dot{\varphi}_1\sin\theta_1\sin\varphi_1\right) + m\left(\dot{z_h} + l\dot{\theta}_1\cos\theta_1\right)\left(-l\dot{\theta}_1\sin\theta_1\right) = -ml\dot{x_h}\left(\dot{\theta}_1\cos\theta_1\cos\varphi_1 -\right.$
$\left.\dot{\varphi}_1\sin\theta_1\sin\varphi_1\right) + ml^2\left(\dot{\theta}_1\sin\theta_1\cos\varphi_1 + \dot{\varphi}_1\cos\theta_1\sin\varphi_1\right)\left(\dot{\theta}_1\cos\theta_1\cos\varphi_1 -\right.$
$\left.\dot{\varphi}_1\sin\theta_1\sin\varphi_1\right) - m\dot{z_h}l\dot{\theta}_1\sin\theta_1 - ml^2{\dot{\theta}_1}^2\cos\theta_1\sin\theta_1 =$

$-ml\dot{x_h}\left(\dot{\theta}_1\cos\theta_1\cos\varphi_1 - \dot{\varphi}_1\sin\theta_1\sin\varphi_1\right)$
$+ ml^2\left({\dot{\theta}_1}^2\sin\theta_1\cos\varphi_1\cos\theta_1\cos\varphi_1 - \dot{\theta}_1\dot{\varphi}_1\sin\theta_1\cos\varphi_1\sin\theta_1\sin\varphi_1\right.$
$\left.+ \dot{\theta}_1\dot{\varphi}_1\cos\theta_1\sin\varphi_1\cos\theta_1\cos\varphi_1 - {\dot{\varphi}_1}^2\cos\theta_1\sin\varphi_1\sin\theta_1\sin\varphi_1\right)$
$- m\dot{z_h}l\dot{\theta}_1\sin\theta_1 - ml^2{\dot{\theta}_1}^2\cos\theta_1\sin\theta_1$

- $\left(\frac{dV}{d\theta_1}\right) = (m_1 - \rho v_1)g(l\cos\theta_1)$

$$\frac{\partial}{\partial t}\left(\frac{dT}{d\dot{\theta}_1}\right) - \left(\frac{dT}{d\theta_1}\right) + \left(\frac{dV}{d\theta_1}\right) =$$

$$\ddot{x_h}(-ml\sin\theta_1\cos\varphi_1) + m\ddot{z_h}l\cos\theta_1 + ml^2\ddot{\theta}_1(\sin\theta_1\cos\varphi_1\sin\theta_1\cos\varphi_1 + \cos\theta_1\cos\theta_1 + J)$$
$$+ ml^2\ddot{\varphi}_1(\cos\theta_1\sin\varphi_1\sin\theta_1\cos\varphi_1) + ml^2{\dot{\varphi}_1}^2(\cos\theta_1\sin\theta_1\cos\varphi_1\cos\varphi_1)$$
$$+ ml^2{\dot{\theta}_1}^2(\cos\theta_1\cos\varphi_1\sin\theta_1\cos\varphi_1 - \cos\theta_1\sin\theta_1)$$
$$+ ml^2\dot{\theta}_1\dot{\varphi}_1(-2\sin\theta_1\sin\varphi_1\sin\theta_1\cos\varphi_1) + (m_1 - \rho v_1)g(l\cos\theta_1)$$

$$\left(\frac{dT}{d\dot{\varphi}_1}\right) = -ml\cos\theta_1\sin\varphi_1\left(\dot{x_h} - l\left(\dot{\theta}_1\sin\theta_1\cos\varphi_1 + \dot{\varphi}_1\cos\theta_1\sin\varphi_1\right)\right)$$
$$+ ml\cos\varphi_1\left(\dot{y_h} + l\dot{\varphi}_1\cos\varphi_1\right) + J\dot{\varphi}_1$$
$$= -ml\dot{x_h}\cos\theta_1\sin\varphi_1$$
$$+ ml^2\left(\dot{\theta}_1\sin\theta_1\cos\varphi_1\cos\theta_1\sin\varphi_1 + \dot{\varphi}_1\cos\theta_1\sin\varphi_1\cos\theta_1\sin\varphi_1\right)$$
$$+ ml\dot{y_h}\cos\varphi_1 + ml^2\dot{\varphi}_1\cos\varphi_1\cos\varphi_1 + J\dot{\varphi}_1$$

- $\frac{\partial}{\partial t}\left(\frac{dT}{d\dot{\varphi}_1}\right) = -ml\ddot{x_h}\cos\theta_1\sin\varphi_1 - ml\dot{x_h}\left(-\dot{\theta}_1\sin\theta_1\sin\varphi_1 + \dot{\varphi}_1\cos\varphi_1\cos\theta_1\right) +$
$ml^2\left(\ddot{\theta_1}\sin\theta_1\cos\varphi_1\cos\theta_1\sin\varphi_1 +\right.$
$\dot{\theta_1}^2\cos\theta_1\cos\varphi_1\cos\theta_1\sin\varphi_1 - \dot{\theta_1}^2\sin\theta_1\cos\varphi_1\sin\theta_1\sin\varphi_1 -$
$\dot{\theta}_1\dot{\varphi}_1\sin\theta_1\sin\varphi_1\cos\theta_1\sin\varphi_1 + \dot{\theta}_1\dot{\varphi}_1\sin\theta_1\cos\varphi_1\cos\theta_1\cos\varphi_1 -$
$2\dot{\varphi}_1\dot{\theta}_1\sin\theta_1\sin\varphi_1\cos\theta_1\sin\varphi_1 +$
$\left.2\varphi_1^2\cos\theta_1\sin\varphi_1\cos\theta_1\cos\varphi_1 + \ddot{\varphi}_1\cos\theta_1\sin\varphi_1\cos\theta_1\sin\varphi_1\right) + ml\ddot{y_h}\cos\varphi_1 -$
$ml\dot{y_h}\dot{\varphi}_1\sin\varphi_1 + ml^2\ddot{\varphi}_1\cos\varphi_1\cos\varphi_1 - 2ml^2\dot{\varphi_1}^2\cos\varphi_1\sin\varphi_1 + J\ddot{\varphi}_1$

$$\left(\frac{dT}{d\varphi_1}\right) = -ml\left(\dot{x_h} - l\left(\dot{\theta}_1\sin\theta_1\cos\varphi_1 + \dot{\varphi}_1\cos\theta_1\sin\varphi_1\right)\right)\left(-\dot{\theta}_1\sin\theta_1\sin\varphi_1\right.$$
$$\left.+ \dot{\varphi}_1\cos\theta_1\cos\varphi_1\right) - ml\dot{\varphi}_1\sin\varphi_1\left(\dot{y_h} + l\dot{\varphi}_1\cos\varphi_1\right)$$
$$= -ml\dot{x_h}\left(-\dot{\theta}_1\sin\theta_1\sin\varphi_1 + \dot{\varphi}_1\cos\theta_1\cos\varphi_1\right)$$
$$+ ml^2\left(-\dot{\theta_1}^2\sin\theta_1\cos\varphi_1\sin\theta_1\sin\varphi_1 + \dot{\theta}_1\dot{\varphi}_1\sin\theta_1\cos\varphi_1\cos\theta_1\cos\varphi_1\right.$$
$$\left.- \dot{\theta}_1\dot{\varphi}_1\cos\theta_1\sin\varphi_1\sin\theta_1\sin\varphi_1 + \dot{\varphi_1}^2\cos\theta_1\sin\varphi_1\cos\theta_1\cos\varphi_1\right)$$

$$-ml\dot{y_h}\dot{\varphi}_1\sin\varphi_1 - ml^2\dot{\varphi_1}^2\sin\varphi_1\cos\varphi_1$$

- $\left(\frac{dV}{d\varphi_1}\right) = 0$

$$\frac{\partial}{\partial t}\left(\frac{dT}{d\dot{\varphi}_1}\right) - \left(\frac{dT}{d\varphi_1}\right) =$$

$$\ddot{x_h}(-ml\cos\theta_1\sin\varphi_1) + \ddot{y_h}(ml\cos\varphi_1) + \ddot{\theta}_1(ml^2\sin\theta_1\cos\varphi_1\cos\theta_1\sin\varphi_1)$$
$$+ \ddot{\varphi}_1(ml^2\cos\theta_1\sin\varphi_1\cos\theta_1\sin\varphi_1 + ml^2\cos\varphi_1\cos\varphi_1 + J)$$
$$+ \dot{\theta_1}^2(ml^2\cos\theta_1\cos\varphi_1\cos\theta_1\sin\varphi_1)$$
$$+ \dot{\varphi_1}^2(ml^2\cos\theta_1\sin\varphi_1\cos\theta_1\cos\varphi_1 - ml^2\sin\varphi_1\cos\varphi_1)$$
$$+ \dot{\theta}_1\dot{\varphi}_1(-2ml^2\sin\theta_1\sin\varphi_1\cos\theta_1\sin\varphi_1)$$

$$\begin{pmatrix} Tx \\ Ty \\ Tz \\ T\varphi_1 \\ T\theta_1 \end{pmatrix} = \begin{pmatrix} 2m & 0 & 0 & -ml\cos\theta_1\sin\varphi_1 & -ml\sin\theta_1\cos\varphi_1 \\ 0 & 2m & 0 & ml\cos\varphi_1 & 0 \\ 0 & 0 & 2m & 0 & ml\cos\theta_1 \\ -ml\cos\theta_1\sin\varphi_1 & ml\cos\varphi_1 & 0 & ml^2\cos\theta_1\sin\varphi_1\cos\theta_1\sin\varphi_1 + ml^2\cos\varphi_1\cos\varphi_1 + J & ml^2\sin\theta_1\cos\varphi_1\cos\theta_1\sin\varphi_1 \\ -ml\sin\theta_1\cos\varphi_1 & 0 & ml\cos\theta_1 & ml^2\cos\theta_1\sin\varphi_1\sin\theta_1\cos\varphi_1 & (ml^2\sin\theta_1\cos\varphi_1\sin\theta_1\cos\varphi_1 + ml^2\cos\theta_1\cos\theta_1 + J) \end{pmatrix} \begin{pmatrix} \ddot{x_h} \\ \ddot{y_h} \\ \ddot{z_h} \\ \ddot{\varphi_1} \\ \ddot{\theta_1} \end{pmatrix}$$
$$+ \begin{pmatrix} 0 & 0 & 0 & -ml\cos\theta_1\cos\varphi_1 & -ml\cos\theta_1\cos\varphi_1 \\ 0 & 0 & 0 & -ml\sin\varphi_1 & 0 \\ 0 & 0 & 0 & 0 & -ml\sin\theta_1 \\ 0 & 0 & 0 & ml^2\cos\theta_1\sin\varphi_1\cos\theta_1\cos\varphi_1 - ml^2\sin\varphi_1\cos\varphi_1 & ml^2\cos\theta_1\cos\varphi_1\cos\theta_1\sin\varphi_1 \\ 0 & 0 & 0 & ml^2\cos\theta_1\sin\theta_1\cos\varphi_1\cos\varphi_1 & (ml^2\cos\theta_1\cos\varphi_1\sin\theta_1\cos\varphi_1 - ml^2\cos\theta_1\sin\theta_1) \end{pmatrix} \begin{pmatrix} \dot{x_h}^2 \\ \dot{y_h}^2 \\ \dot{z_h}^2 \\ \dot{\varphi_1}^2 \\ \dot{\theta_1}^2 \end{pmatrix}$$
$$+ \begin{pmatrix} 0 & 0 & 0 & 2ml\dot{\theta_1}\dot{\varphi_1}\sin\theta_1\sin\varphi_1 & 0 \\ 0 & 0 & 0 & 0 & 0 \\ 0 & 0 & 0 & 0 & 0 \\ 0 & 0 & 0 & -2ml^2\sin\theta_1\sin\varphi_1\cos\theta_1\sin\varphi_1 & 0 \\ 0 & 0 & 0 & 0 & -2ml^2\sin\theta_1\sin\varphi_1\sin\theta_1\cos\varphi_1 \end{pmatrix} \begin{pmatrix} 0 \\ 0 \\ 0 \\ \dot{\varphi_1}\dot{\theta_1} \\ \dot{\theta_1}\dot{\varphi_1} \end{pmatrix} + \begin{pmatrix} 0 \\ 0 \\ (m_0 - \rho v_0)g + (m_1 - \rho v_1)g \\ (m_1 - \rho v_1)g(l\cos\theta_1) \\ 0 \end{pmatrix} + D + MA = AF$$

Forces derivation (first 3 links)

$$F\frac{\mathrm{dP}}{\mathrm{dq}} = F_1\frac{dP}{dq} + F_2\frac{dP}{dq} + F_3\frac{dP}{dq} + F_4\frac{dP}{dq}$$

$$F_1 = \begin{bmatrix} Fx \\ 0 \\ 0 \end{bmatrix} F_2 = \begin{bmatrix} Fx \\ 0 \\ 0 \end{bmatrix} F_3 = \begin{bmatrix} 0 \\ 0 \\ Fz \end{bmatrix} F_4 = \begin{bmatrix} 0 \\ 0 \\ Fz \end{bmatrix}$$

$$x_n = x_h + 2l + \sum_{i=2}^{N-1} 2l\cos\theta_i\cos\varphi_i + l\cos\theta_n\cos\varphi_n$$

$$y_n = y_h + \sum_{i=2}^{N-1} 2l\sin\varphi_i + l\sin\varphi_n$$

$$z_n = z_h + \sum_{i=2}^{N-1} 2l\sin\theta_i + l\sin\theta_n$$

- $at \;\; x_h$:

$$F_1\frac{dx1}{dx_h} + F_2\frac{dx1}{dx_h} + F_3\frac{dx2}{dx_h} + F_4\frac{dx2}{dx_h}$$

$$F_1\begin{bmatrix}\cos(\theta_1)\cos(\varphi_1) & -\sin(\varphi_1)\cos(\theta_1) & \sin(\theta_1)\\ \sin(\varphi_1) & \cos(\varphi_1) & 0\\ \cos(\varphi_1)\sin(\theta_1) & \sin(\varphi_1)\sin(\theta_1) & \cos(\theta_1)\end{bmatrix}\frac{d}{dx_h}\begin{bmatrix}x_h+2l+l\cos\theta_1\cos\varphi_1\\ y_h+l\sin\varphi_1\\ z_h+l\sin\theta_1\end{bmatrix}$$
$$+F_2R1\frac{d}{dx_h}\begin{bmatrix}x_h+2l+l\cos\theta_1\cos\varphi_1\\ y_h+l\sin\varphi_1\\ z_h+l\sin\theta_1\end{bmatrix}F_3R2\frac{d}{dx_h}\begin{bmatrix}x_h+2l+2l\cos\theta_1\cos\varphi_1+l\cos\theta_2\cos\varphi_2\\ y_h+2l\sin\varphi_1+l\sin\varphi_2\\ z_h+2l\sin\theta_1+l\sin\theta_2\end{bmatrix}$$
$$+F_4\begin{bmatrix}\cos(\theta_2)\cos(\varphi_2) & -\sin(\varphi_2)\cos(\theta_2) & \sin(\theta_2)\\ \sin(\varphi_1) & \cos(\varphi_1) & 0\\ \cos(\varphi_2)\sin(\theta_2) & \sin(\varphi_2)\sin(\theta_2) & \cos(\theta_2)\end{bmatrix}\frac{d}{dx_h}\begin{bmatrix}x_h+2l+2l\cos\theta_1\cos\varphi_1+l\cos\theta_2\cos\varphi_2\\ y_h+2l\sin\varphi_1+l\sin\varphi_2\\ z_h+2l\sin\theta_1+l\sin\theta_2\end{bmatrix}$$

$$F_1R\begin{bmatrix}1\\0\\0\end{bmatrix}+F_2R\begin{bmatrix}1\\0\\0\end{bmatrix}+F_3R\begin{bmatrix}0\\0\\0\end{bmatrix}+F_4R\begin{bmatrix}0\\0\\0\end{bmatrix}=$$

$$F_1\begin{bmatrix}\cos(\theta_1)\cos(\varphi_1)\\ \sin(\varphi_1)\\ \cos(\varphi_1)\sin(\theta_1)\end{bmatrix}+F_2\begin{bmatrix}\cos(\theta_1)\cos(\varphi_1)\\ \sin(\varphi_1)\\ \cos(\varphi_1)\sin(\theta_1)\end{bmatrix}=2F_x(\cos(\theta_1)\cos(\varphi_1))$$

- $at\ \ y_h$:

$$F_1R\begin{bmatrix}0\\0\\0\end{bmatrix}+F_2R\begin{bmatrix}0\\0\\0\end{bmatrix}+F_3R\begin{bmatrix}0\\0\\0\end{bmatrix}+F_4R\begin{bmatrix}0\\0\\0\end{bmatrix}=0$$

- $at\ \ z_h$:

$$F_3\begin{bmatrix}\cos(\theta_2)\cos(\varphi_2)\\ \sin(\varphi_1)\\ \cos(\varphi_2)\sin(\theta_2)\end{bmatrix}+F_4\begin{bmatrix}\cos(\theta_2)\cos(\varphi_2)\\ \sin(\varphi_1)\\ \cos(\varphi_2)\sin(\theta_2)\end{bmatrix}=2F_{3z}(\cos(\varphi_2)\sin(\theta_2))$$

- $at\ \theta_1$:

$$F\frac{\mathrm{dP}}{\mathrm{d}\theta_1}=F_1\frac{dx1}{d\theta_1}+F_2\frac{dx1}{d\theta_1}+F_3\frac{dx2}{d\theta_1}+F_4\frac{dx2}{d\theta_1}$$

$$F_1\begin{bmatrix}\cos(\theta_1)\cos(\varphi_1) & -\sin(\varphi_1)\cos(\theta_1) & \sin(\theta_1)\\ \sin(\varphi_1) & \cos(\varphi_1) & 0\\ \cos(\varphi_1)\sin(\theta_1) & \sin(\varphi_1)\sin(\theta_1) & \cos(\theta_1)\end{bmatrix}\frac{d}{d\theta_1}\begin{bmatrix}x_h+2l+l\cos\theta_1\cos\varphi_1\\ y_h+l\sin\varphi_1\\ z_h+l\sin\theta_1\end{bmatrix}^T$$
$$+F_2R\frac{d}{d\theta_1}\begin{bmatrix}x_h+2l+l\cos\theta_1\cos\varphi_1\\ y_h+l\sin\varphi_1\\ z_h+l\sin\theta_1\end{bmatrix}^T$$
$$+F_3\begin{bmatrix}\cos(\theta_2)\cos(\varphi_2) & -\sin(\varphi_2)\cos(\theta_2) & \sin(\theta_2)\\ \sin(\varphi_1) & \cos(\varphi_1) & 0\\ \cos(\varphi_2)\sin(\theta_2) & \sin(\varphi_2)\sin(\theta_2) & \cos(\theta_2)\end{bmatrix}\frac{d}{d\theta_1}\begin{bmatrix}x_h+2l+2l\cos\theta_1\cos\varphi_1+l\cos\theta_2\cos\varphi_2\\ y_h+2l\sin\varphi_1+l\sin\varphi_2\\ z_h+2l\sin\theta_1+l\sin\theta_2\end{bmatrix}$$
$$+F_3R\frac{d}{d\theta_1}\begin{bmatrix}x_h+2l+2l\cos\theta_1\cos\varphi_1+l\cos\theta_2\cos\varphi_2\\ y_h+2l\sin\varphi_1+l\sin\varphi_2\\ z_h+2l\sin\theta_1+l\sin\theta_2\end{bmatrix}$$

$$F_1R\begin{bmatrix}-l\sin\theta_1\cos\varphi_1\\ 0\\ l\cos\theta_1\end{bmatrix}+F_2R\begin{bmatrix}-l\sin\theta_1\cos\varphi_1\\ 0\\ l\cos\theta_1\end{bmatrix}+$$
$$F_3R\begin{bmatrix}-2l\cos\theta_1\sin\varphi_1\\ 0\\ 2l\cos\theta_1\end{bmatrix}+F_4R\begin{bmatrix}-2l\cos\theta_1\sin\varphi_1\\ 0\\ 2l\cos\theta_1\end{bmatrix}=$$

$$[Fx\quad 0\quad 0]\begin{bmatrix}-l\sin\theta_1\cos\varphi_1\\ 0\\ l\cos\theta_1\end{bmatrix}+[Fx\quad 0\quad 0]\begin{bmatrix}-l\sin\theta_1\cos\varphi_1\\ 0\\ l\cos\theta_1\end{bmatrix}$$
$$+[0\quad 0\quad Fz]\begin{bmatrix}-2l\cos\theta_1\sin\varphi_1\\ 0\\ 2l\cos\theta_1\end{bmatrix}+[0\quad 0\quad Fz]\begin{bmatrix}-2l\cos\theta_1\sin\varphi_1\\ 0\\ 2l\cos\theta_1\end{bmatrix}$$
$$Fx\left(\frac{lsin(2\varphi_1-2\theta_1)+2lsin(2\theta_1)-lsin(2\varphi_1+2\theta_1)}{8}\right)+Fz$$

- $at\ \varphi_1$:

$$F\frac{\mathrm{dP}}{\mathrm{d}\varphi_1}=F_1\frac{dx1}{d\varphi_1}+F_2\frac{dx1}{d\varphi_1}+F_3\frac{dx2}{d\varphi_1}+F_4\frac{dx2}{d\varphi_1}$$

$$F_1 \frac{d}{d\varphi_1}\begin{bmatrix} x_h + 2l + l\cos\theta_1\cos\varphi_1 \\ y_h + l\sin\varphi_1 \\ z_h + l\sin\theta_1 \end{bmatrix} + F_2 \frac{d}{d\varphi_1}\begin{bmatrix} x_h + 2l + l\cos\theta_1\cos\varphi_1 \\ y_h + l\sin\varphi_1 \\ z_h + l\sin\theta_1 \end{bmatrix}$$
$$+ F_3 \frac{d}{d\varphi_1}\begin{bmatrix} x_h + 2l + 2l\cos\theta_1\cos\varphi_1 + l\cos\theta_2\cos\varphi_2 \\ y_h + 2l\sin\varphi_1 + l\sin\varphi_2 \\ z_h + 2l\sin\theta_1 + l\sin\theta_2 \end{bmatrix}$$
$$+ F_4 \frac{d}{d\varphi_1}\begin{bmatrix} x_h + 2l + 2l\cos\theta_1\cos\varphi_1 + l\cos\theta_2\cos\varphi_2 \\ y_h + 2l\sin\varphi_1 + l\sin\varphi_2 \\ z_h + 2l\sin\theta_1 + l\sin\theta_2 \end{bmatrix}$$

$$F_1\begin{bmatrix} -l\cos\theta_1\sin\varphi_1 \\ l\cos\varphi_1 \\ 0 \end{bmatrix} + F_2\begin{bmatrix} -l\cos\theta_1\sin\varphi_1 \\ l\cos\varphi_1 \\ 0 \end{bmatrix} + F_3\begin{bmatrix} -2l\cos\theta_1\sin\varphi_1 \\ 2l\cos\varphi_1 \\ 0 \end{bmatrix} + F_4\begin{bmatrix} -2l\cos\theta_1\sin\varphi_1 \\ 2l\cos\varphi_1 \\ 0 \end{bmatrix}$$

$$F\frac{\mathrm{dP}}{\mathrm{d}\varphi_2} = F_1\frac{dx1}{d\varphi_2} + F_2\frac{dx1}{d\varphi_2} + F_3\frac{dx2}{d\varphi_2} + F_4\frac{dx2}{d\varphi_2}$$

$$F_1\frac{d}{d\varphi_2}\begin{bmatrix} 0 \\ 0 \\ 0 \end{bmatrix} + F_2\frac{d}{d\varphi_2}\begin{bmatrix} 0 \\ 0 \\ 0 \end{bmatrix} + F_3\frac{d}{d\varphi_2}\begin{bmatrix} -l\cos\theta_2\sin\varphi_2 \\ l\cos\varphi_2 \\ 0 \end{bmatrix} + F_4\frac{d}{d\varphi_2}\begin{bmatrix} -l\cos\theta_2\sin\varphi_2 \\ l\cos\varphi_2 \\ 0 \end{bmatrix}$$

C. Manual derivation of the configuration matrix

$$
T = \begin{bmatrix}
\sin\boldsymbol{\theta_1} & \sin\boldsymbol{\theta_1} \\
0 & 0 \\
\cos\boldsymbol{\theta_1} & \cos\boldsymbol{\theta_1} \\
\cos\boldsymbol{\theta_1}\left(d + l.\frac{\sin\boldsymbol{\psi_1}}{\mathbf{2}} + l.\sin\boldsymbol{\psi_2} + \boldsymbol{l}.\sin\boldsymbol{\psi_3}\right) & -\cos\boldsymbol{\theta_1}\left(d + l.\frac{\sin\boldsymbol{\psi_1}}{\mathbf{2}} + l.\sin\boldsymbol{\psi_2} + \boldsymbol{l}.\sin\boldsymbol{\psi_3}\right) \quad \dots \\
-\mathrm{l}.\sin\boldsymbol{\theta_1}\left(\frac{\cos\boldsymbol{\theta_1}}{\mathbf{2}} + \cos\boldsymbol{\theta_2} + \cos\boldsymbol{\theta_3}\right) & -\mathrm{l}.\sin\boldsymbol{\theta_1}\left(\frac{\cos\boldsymbol{\theta_1}}{\mathbf{2}} + \cos\boldsymbol{\theta_2} + \cos\boldsymbol{\theta_3}\right) \\
0 & 0 \\
\cos\boldsymbol{\theta_2}.\cos\boldsymbol{\psi_2} & \cos\boldsymbol{\theta_2}.\cos\boldsymbol{\psi_2} \\
-\sin\boldsymbol{\psi_2} & -\sin\boldsymbol{\psi_2} \\
\sin\boldsymbol{\theta_2} & \sin\boldsymbol{\theta_2} \\
-\left(d + l.\frac{\sin\boldsymbol{\psi_2}}{\mathbf{2}} + \boldsymbol{l}.\sin\boldsymbol{\psi_3}\right)\sin\boldsymbol{\theta_2} & \left(d + l.\frac{\sin\boldsymbol{\psi_2}}{\mathbf{2}} + \boldsymbol{l}.\sin\boldsymbol{\psi_3}\right)\sin\boldsymbol{\theta_2} \quad \dots \\
\mathrm{l}.\cos\boldsymbol{\theta_2}\left(\frac{\sin\boldsymbol{\theta_2}}{\mathbf{2}} + \sin\boldsymbol{\theta_3}\right) - \mathrm{l}.\sin\boldsymbol{\theta_2}\left(\frac{\cos\boldsymbol{\theta_2}}{\mathbf{2}} + \cos\boldsymbol{\theta_3}\right) & \mathrm{l}.\cos\boldsymbol{\theta_2}\left(\frac{\sin\boldsymbol{\theta_2}}{\mathbf{2}} + \sin\boldsymbol{\theta_3}\right) - \mathrm{l}.\sin\boldsymbol{\theta_2}\left(\frac{\cos\boldsymbol{\theta_2}}{\mathbf{2}} + \cos\boldsymbol{\theta_3}\right) \\
l.\cos\boldsymbol{\psi_2}\left(\frac{\cos\boldsymbol{\psi_2}}{\mathbf{2}} + \cos\boldsymbol{\psi_3}\right) - l.\sin\boldsymbol{\psi_2}\left(\frac{\sin\boldsymbol{\psi_2}}{\mathbf{2}} + \sin\boldsymbol{\psi_3}\right) & l.\cos\boldsymbol{\psi_2}\left(\frac{\cos\boldsymbol{\psi_2}}{\mathbf{2}} + \cos\boldsymbol{\psi_3}\right) + l.\sin\boldsymbol{\psi_2}\left(\frac{\sin\boldsymbol{\psi_2}}{\mathbf{2}} + \sin\boldsymbol{\psi_3}\right) \\
-\sin\boldsymbol{\psi_3} & -\sin\boldsymbol{\psi_3} \\
\cos\boldsymbol{\psi_3} & \cos\boldsymbol{\psi_3} \\
0 & 0 \\
NA & NA \quad \dots \\
0 & 0 \\
\left(-\frac{3}{4}.\mathrm{l}.\cos\boldsymbol{\psi_3}.\cos\boldsymbol{\psi_3} + \frac{3}{4}.l.\sin\boldsymbol{\psi_3}.\sin\boldsymbol{\psi_3}\right).\frac{3}{4}.l.\cos\boldsymbol{\theta_3} & \left(-\frac{1}{4}.\mathrm{l}.\cos\boldsymbol{\psi_3}.\cos\boldsymbol{\psi_3} + \frac{1}{4}.l.\sin\boldsymbol{\psi_3}.\sin\boldsymbol{\psi_3}\right).\frac{1}{4}.l.\cos\boldsymbol{\theta_3} \\
-\sin\boldsymbol{\psi_4} & -\sin\boldsymbol{\psi_4} \\
\cos\boldsymbol{\psi_4} & \cos\boldsymbol{\psi_4} \\
0 & 0 \\
NA & NA \quad \dots \\
0 & 0 \\
\left(+\frac{3}{4}.\mathrm{l}.\cos\boldsymbol{\psi_4}.\cos\boldsymbol{\psi_4} - \frac{3}{4}.l.\sin\boldsymbol{\psi_4}.\sin\boldsymbol{\psi_4}\right).\frac{3}{4}.l.\cos\boldsymbol{\theta_4} & \left(+\frac{1}{4}.\mathrm{l}.\cos\boldsymbol{\psi_4}.\cos\boldsymbol{\psi_4} - \frac{1}{4}.l.\sin\boldsymbol{\psi_4}.\sin\boldsymbol{\psi_4}\right).\frac{1}{4}.l.\cos\boldsymbol{\theta_4} \\
\cos\boldsymbol{\theta_5}.\cos\boldsymbol{\psi_5} & \cos\boldsymbol{\theta_5}.\cos\boldsymbol{\psi_5} \\
-\sin\boldsymbol{\psi_5} & -\sin\boldsymbol{\psi_5} \\
\sin\boldsymbol{\theta_5} & \sin\boldsymbol{\theta_5} \\
-\left(d + l.\frac{\sin\boldsymbol{\psi_5}}{\mathbf{2}} + \boldsymbol{l}.\sin\boldsymbol{\psi_4}\right)\sin\boldsymbol{\theta_5} & \left(d + l.\frac{\sin\boldsymbol{\psi_5}}{\mathbf{2}} + \boldsymbol{l}.\sin\boldsymbol{\psi_4}\right)\sin\boldsymbol{\theta_5} \quad \dots \\
-\mathrm{l}.\cos\boldsymbol{\theta_5}\left(\frac{\sin\boldsymbol{\theta_5}}{\mathbf{2}} + \sin\boldsymbol{\theta_4}\right) + \mathrm{l}.\sin\boldsymbol{\theta_5}\left(\frac{\cos\boldsymbol{\theta_5}}{\mathbf{2}} + \cos\boldsymbol{\theta_4}\right) & -\mathrm{l}.\cos\boldsymbol{\theta_5}\left(\frac{\sin\boldsymbol{\theta_5}}{\mathbf{2}} + \sin\boldsymbol{\theta_4}\right) + \mathrm{l}.\sin\boldsymbol{\theta_5}\left(\frac{\cos\boldsymbol{\theta_5}}{\mathbf{2}} + \cos\boldsymbol{\theta_4}\right) \\
-l.\cos\boldsymbol{\psi_5}\left(\frac{\cos\boldsymbol{\psi_5}}{\mathbf{2}} + \cos\boldsymbol{\psi_4}\right) + l.\sin\boldsymbol{\psi_5}\left(\frac{\sin\boldsymbol{\psi_5}}{\mathbf{2}} + \sin\boldsymbol{\psi_4}\right) & -l.\cos\boldsymbol{\psi_5}\left(\frac{\cos\boldsymbol{\psi_5}}{\mathbf{2}} + \cos\boldsymbol{\psi_4}\right) - l.\sin\boldsymbol{\psi_5}\left(\frac{\sin\boldsymbol{\psi_5}}{\mathbf{2}} + \sin\boldsymbol{\psi_4}\right) \\
\sin\boldsymbol{\theta_6} & \sin\boldsymbol{\theta_6} \\
0 & 0 \\
\cos\boldsymbol{\theta_6} & \cos\boldsymbol{\theta_6} \\
\cos\boldsymbol{\theta_6}\left(d + l.\frac{\sin\boldsymbol{\psi_6}}{\mathbf{2}} + l.\sin\boldsymbol{\psi_5} + \boldsymbol{l}.\sin\boldsymbol{\psi_4}\right) & \cos\boldsymbol{\theta_6}\left(d + l.\frac{\sin\boldsymbol{\psi_6}}{\mathbf{2}} + l.\sin\boldsymbol{\psi_5} + \boldsymbol{l}.\sin\boldsymbol{\psi_4}\right) \\
+\mathrm{l}.\sin\boldsymbol{\theta_6}\left(\frac{\cos\boldsymbol{\theta_6}}{\mathbf{2}} + \cos\boldsymbol{\theta_5} + \cos\boldsymbol{\theta_4}\right) & +\mathrm{l}.\sin\boldsymbol{\theta_6}\left(\frac{\cos\boldsymbol{\theta_6}}{\mathbf{2}} + \cos\boldsymbol{\theta_5} + \cos\boldsymbol{\theta_4}\right) \\
0 & 0
\end{bmatrix}
\begin{bmatrix} f_1 \\ f_2 \\ f_3 \\ f_4 \\ f_5 \\ f_6 \\ f_7 \\ f_8 \\ f_9 \\ f_{10} \\ f_{11} \\ f_{12} \end{bmatrix}
$$

8x12 matrix * 12x1 matrix

D. Hydrodynamics derived equations

$$M_{RB} = \begin{bmatrix} m & 0 & 0 & 0 & mz_g & -my_g \\ 0 & m & 0 & -mz_g & 0 & mx_g \\ 0 & 0 & m & my_g & -mx_g & 0 \\ 0 & -mz_g & my_g & I_x & -I_{xy} & -I_{xz} \\ mz_g & 0 & -mx_g & -I_{yx} & I_y & -I_{yz} \\ -my_g & mx_g & 0 & -I_{zx} & -I_{zy} & I_z \end{bmatrix}$$

$$C_{RB} = \begin{bmatrix} 0 & 0 & 0 & m(y_g q + z_g r) & -m(x_g q - w) & -m(x_g r + v) \\ 0 & 0 & 0 & -m(y_g p + w) & m(z_g r + x_g p) & -m(y_g r - u) \\ 0 & 0 & 0 & -m(z_g p - v) & -m(z_g q + u) & m(x_g p + y_g q) \\ -m(y_g q + z_g r) & m(y_g p + w) & m(z_g p - v) & 0 & -I_{yz} q - I_{xz} p + I_z r & I_{yz} r + I_{xy} p - I_y q \\ m(x_g q - w) & -m(z_g r + x_g p) & m(z_g q + u) & I_{yz} q + I_{xz} p - I_z r & 0 & -I_{xz} r - I_{xy} q + I_x p \\ m(x_g r + v) & m(y_g r - u) & -m(x_g p + y_g q) & -I_{yz} r - I_{xy} p + I_y q & I_{xz} r + I_{xy} q - I_x p & 0 \end{bmatrix}$$

$$g(\eta) = \begin{bmatrix} (W - B)\sin(\theta) \\ -(W - B)\cos(\theta)\sin(\Phi) \\ -(W - B)\cos(\theta)\sin(\Phi) \\ -(y_g W - y_b B)\cos(\theta)\sin(\Phi) + (z_g W - z_b B)\cos(\theta)\sin(\Phi) \\ (z_g W - z_b B)\sin(\theta) + (x_g W - x_b B)\cos(\theta)\cos(\Phi) \\ -(x_g W - x_b B)\cos(\theta)\sin(\Phi) - (y_g W - y_b B)\sin(\theta) \end{bmatrix}$$

$$M_A = - \begin{bmatrix} X_{\dot{u}} & X_{\dot{v}} & X_{\dot{w}} & X_{\dot{p}} & X_{\dot{q}} & X_{\dot{r}} \\ Y_{\dot{u}} & Y_{\dot{v}} & Y_{\dot{w}} & Y_{\dot{p}} & Y_{\dot{q}} & Y_{\dot{r}} \\ Z_{\dot{u}} & Z_{\dot{v}} & Z_{\dot{w}} & Z_{\dot{p}} & Z_{\dot{q}} & Z_{\dot{r}} \\ K_{\dot{u}} & K_{\dot{v}} & K_{\dot{w}} & K_{\dot{p}} & K_{\dot{q}} & K_{\dot{r}} \\ M_{\dot{u}} & M_{\dot{v}} & M_{\dot{w}} & M_{\dot{p}} & M_{\dot{q}} & M_{\dot{r}} \\ N_{\dot{u}} & N_{\dot{v}} & N_{\dot{w}} & N_{\dot{p}} & N_{\dot{q}} & N_{\dot{r}} \end{bmatrix}$$

Where :

$$X_A = X_{\dot{u}}.\dot{u} + X_{\dot{w}}.(\dot{w} + uq) + X_{\dot{q}}.\dot{q} + Z_{\dot{w}}.wq + Z_{\dot{q}}.q^2 + X_{\dot{v}}.\dot{v} + X_{\dot{p}}.\dot{p} + X_{\dot{r}}.\dot{r} - Y_{\dot{v}}.vr - Y_{\dot{p}}.rp - Y_{\dot{r}}.r^2 - X_{\dot{v}}.ur - Y_{\dot{w}}.wr + Y_{\dot{w}}.vq + Z_{\dot{p}}.pq - (Y_{\dot{q}} - Z_{\dot{r}})qr$$

$$Y_A = X_{\dot{v}}.\dot{u} + Y_{\dot{w}}.\dot{w} + Y_{\dot{q}}.\dot{q} + Y_{\dot{v}}.\dot{v} + Y_{\dot{p}}.\dot{p} + Y_{\dot{r}}.\dot{r} + X_{\dot{v}}.vr - Y_{\dot{w}}.vp + X_{\dot{r}}.r^2 + (X_{\dot{p}} - Z_{\dot{r}})rp - Z_{\dot{p}}.p^2 - X_{\dot{w}}(up - wr) + X_{\dot{u}}.ur - Z_{\dot{w}}.wp - Z_{\dot{q}}.pq + X_{\dot{q}}.qr$$

$$Z_A = X_{\dot{w}}.(\dot{u} - wq) + Z_{\dot{w}}.\dot{w} + Z_{\dot{q}}.\dot{q} - X_{\dot{u}}.uq - X_{\dot{q}}.q^2 + Y_{\dot{w}}.\dot{v} + Z_{\dot{p}}.\dot{p} + Z_{\dot{r}}.\dot{r} + Y_{\dot{v}}.vp + Y_{\dot{r}}.rp + Y_{\dot{p}}.p^2 + X_{\dot{v}}.up + Y_{\dot{w}}.wp - X_{\dot{v}}.vq - (X_{\dot{p}} - Y_{\dot{q}})pq - X_{\dot{r}}.qr$$

$$K_A = X_{\dot{p}}.\dot{u} + Z_{\dot{p}}.\dot{w} + K_{\dot{q}}.\dot{q} - X_{\dot{v}}.wu + X_{\dot{r}}.uq - Y_{\dot{w}}.w^2 - (Y_{\dot{q}} - Z_{\dot{r}})wq + M_{\dot{r}}.q^2 + Y_{\dot{p}}.\dot{v} + K_{\dot{p}}.\dot{p} + K_{\dot{r}}.\dot{r} + Y_{\dot{w}}.v^2 - (Y_{\dot{q}} - Z_{\dot{r}})vr + Z_{\dot{p}}.vp - M_{\dot{r}}.r^2 - K_{\dot{q}}.rp + X_{\dot{w}}.uv - (Y_{\dot{v}} - Z_{\dot{w}})vw - (Y_{\dot{r}} + Z_{\dot{q}})wr - Y_{\dot{p}}.wp - X_{\dot{q}}.ur + (Y_{\dot{r}} + Z_{\dot{q}})vq + K_{\dot{r}}.pq - (M_{\dot{q}} - N_{\dot{r}})qr$$

$$M_A = X_{\dot{q}}.(\dot{u} + wq) + Z_{\dot{q}}.(\dot{w} - uq) + M_{\dot{q}}.\dot{q} - X_{\dot{w}}.(u^2 - w^2) - (Z_{\dot{w}} - X_{\dot{u}})wu + Y_{\dot{q}}.\dot{v} + K_{\dot{q}}.\dot{p} + M_{\dot{r}}.\dot{r} - Y_{\dot{r}}.vp + Y_{\dot{p}}.vr - K_{\dot{r}}.(p^2 - r^2) + (K_{\dot{p}} - N_{\dot{r}})rp - Y_{\dot{w}}.uv + X_{\dot{v}}.vw - (X_{\dot{r}} + Z_{\dot{p}}).(up - wr) + (X_{\dot{p}} - Z_{\dot{r}}).(wp + ur) - M_{\dot{r}}.pq + K_{\dot{q}}.q$$

$$N_A = X_{\dot{r}}.\dot{u} + Z_{\dot{r}}.\dot{w} + M_{\dot{r}}.\dot{q} + X_{\dot{v}}.u^2 + Y_{\dot{w}}.wu - (X_{\dot{p}} - Y_{\dot{q}})uq - Z_{\dot{p}}.wq - K_{\dot{q}}.q^2 + Y_{\dot{r}}.\dot{v} + K_{\dot{r}}.\dot{p} + N_{\dot{r}}.\dot{r} - X_{\dot{v}}.v^2 - X_{\dot{r}}.vr - (X_{\dot{p}} - Y_{\dot{q}})vp + M_{\dot{r}}.rp + K_{\dot{q}}.p^2 - (K_{\dot{p}} - M_{\dot{q}})pq - K_{\dot{r}}.qr - (X_{\dot{u}} - Y_{\dot{v}})uv - X_{\dot{w}}.vw + (X_{\dot{q}} + Y_{\dot{p}})up + Y_{\dot{r}}.ur + Z_{\dot{q}}.wp - (X_{\dot{q}} + Y_{\dot{p}})vq$$

$$C_A(v) = \begin{bmatrix} 0 & 0 & 0 & 0 & -a3 & a2 \\ 0 & 0 & 0 & a3 & 0 & -a1 \\ 0 & 0 & 0 & -a2 & a1 & 0 \\ 0 & -a3 & a2 & 0 & -b3 & b2 \\ a3 & 0 & -a1 & b3 & 0 & -b1 \\ -a2 & a1 & 0 & -b2 & b1 & 0 \end{bmatrix}$$

$$a1 = X_{\dot{u}}.u + X_{\dot{v}}.v + X_{\dot{w}}.w + X_{\dot{p}}.p + X_{\dot{q}}.q + X_{\dot{r}}.r$$

$$a2 = X_{\dot{v}}.u + Y_{\dot{v}}.v + Y_{\dot{w}}.w + Y_{\dot{p}}.p + Y_{\dot{q}}.q + Y_{\dot{r}}.r$$

$$a3 = X_{\dot{w}}.u + Y_{\dot{w}}.v + Z_{\dot{w}}.w + Z_{\dot{p}}.p + Z_{\dot{q}}.q + Z_{\dot{r}}.r$$

$$b1 = X_{\dot{p}}.u + Y_{\dot{p}}.v + Z_{\dot{p}}.w + K_{\dot{p}}.p + K_{\dot{q}}.q + K_{\dot{r}}.r$$

$$b2 = X_{\dot{q}}.u + Y_{\dot{q}}.v + Z_{\dot{q}}.w + K_{\dot{q}}.p + M_{\dot{q}}.q + M_{\dot{r}}.r$$

$$b3 = X_{\dot{r}}.u + Y_{\dot{r}}.v + Z_{\dot{r}}.w + K_{\dot{r}}.p + M_{\dot{r}}.q + N_{\dot{r}}.r$$

E. MATLAB results

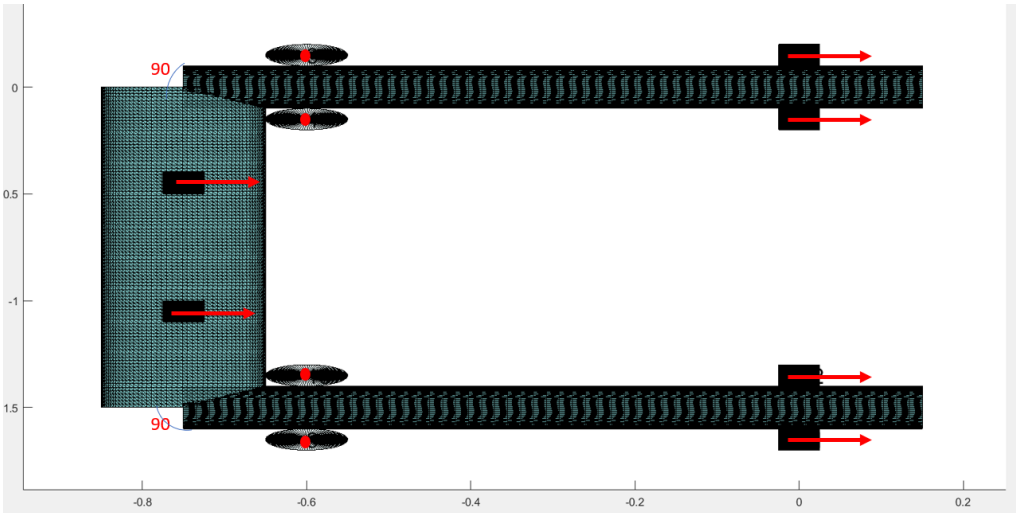

Figure 19 U turn shape

```
Matrix_A =

    1.0000    1.0000         0         0   -1.0000   -1.0000   -1.0000   -1.0000   -0.0000   -0.0000   -1.0000   -1.0000
         0         0         0         0         0         0         0         0         0         0         0         0
         0         0   -1.0000   -1.0000         0         0         0         0   -1.0000   -1.0000         0         0
         0         0   -0.1500    0.1500   -0.0000    0.0000   -0.0000    0.0000    1.6500    1.3500         0         0
         0         0   -0.6000   -0.6000   -0.1500    0.1500   -0.1500    0.1500   -0.6000   -0.6000         0         0
   -0.1500    0.1500   -0.0000    0.0000   -0.4500   -0.4500   -1.0500   -1.0500   -0.0000   -0.0000   -1.6500   -1.3500


algorithm =

   16.0000
    0.0000
   16.0000
    9.0000
    5.7600
   36.0000


rank =

     5
```

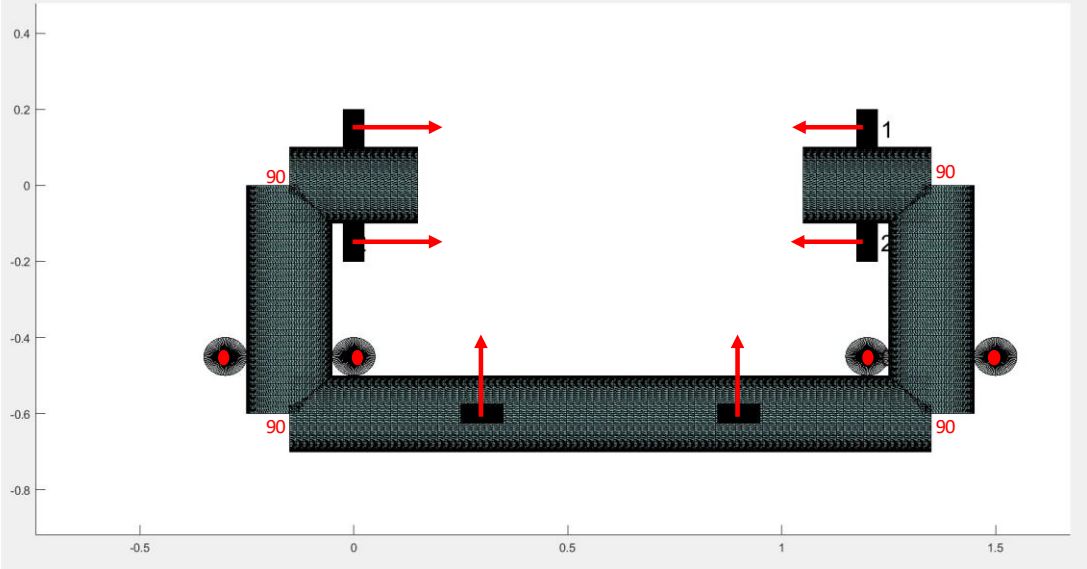

Figure 20 O shape

```
Matrix_A =

    1.0000    1.0000         0         0   -0.0000   -0.0000   -0.0000   -0.0000    0.0000    0.0000    1.0000    1.0000
         0         0    0.0000    0.0000   -1.0000   -1.0000   -1.0000   -1.0000   -0.0000   -0.0000   -0.0000   -0.0000
         0         0   -1.0000   -1.0000         0         0         0         0   -1.0000   -1.0000         0         0
         0         0    0.4500    0.4500    0.1500   -0.1500    0.1500   -0.1500    0.4500    0.4500         0         0
         0         0   -0.3000   -0.0000   -0.0000    0.0000   -0.0000    0.0000    1.5000    1.2000         0         0
   -0.1500    0.1500   -0.0000   -0.0000   -0.3000   -0.3000   -0.9000   -0.9000   -0.0000   -0.0000   -0.1500    0.1500


algorithm =

   16.0000
   16.0000
   16.0000
    3.2400
    5.7600
    5.7600


rank =

     6
```

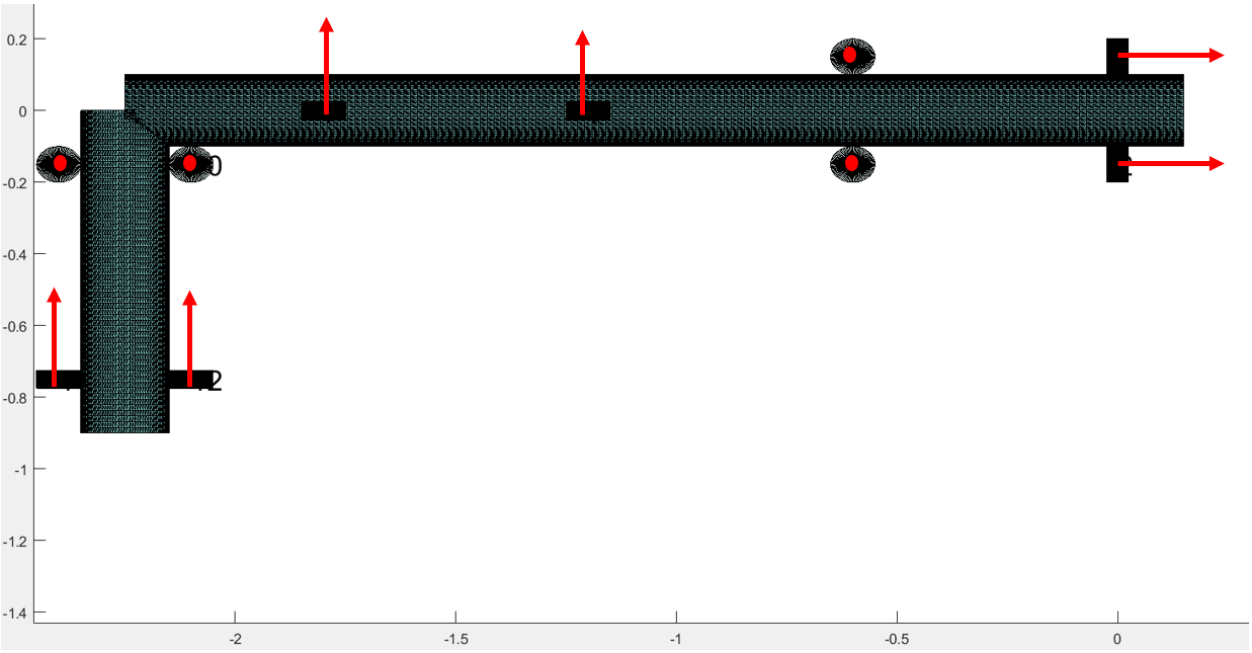

Figure 21 L shape configuration

```
Matrix_A =

    1.0000    1.0000    0.0000    0.0000    0.0000    0.0000    0.0000    0.0000         0         0    0.0000    0.0000
         0         0         0         0    1.0000    1.0000    1.0000    1.0000    0.0000    0.0000    1.0000    1.0000
         0         0   -1.0000   -1.0000         0         0         0         0   -1.0000   -1.0000         0         0
         0         0   -0.1500    0.1500   -0.1500    0.1500   -0.1500    0.1500    0.1500    0.1500         0         0
         0         0   -0.6000   -0.6000    0.0000   -0.0000    0.0000   -0.0000   -2.4000   -2.1000         0         0
   -0.1500    0.1500   -0.0000    0.0000   -1.2000   -1.2000   -1.8000   -1.8000   -0.0000   -0.0000   -2.4000   -2.1000


algorithm =

    4.0000
   36.0000
   16.0000
    0.0900
   32.4900
  110.2500


rank =

     5
```

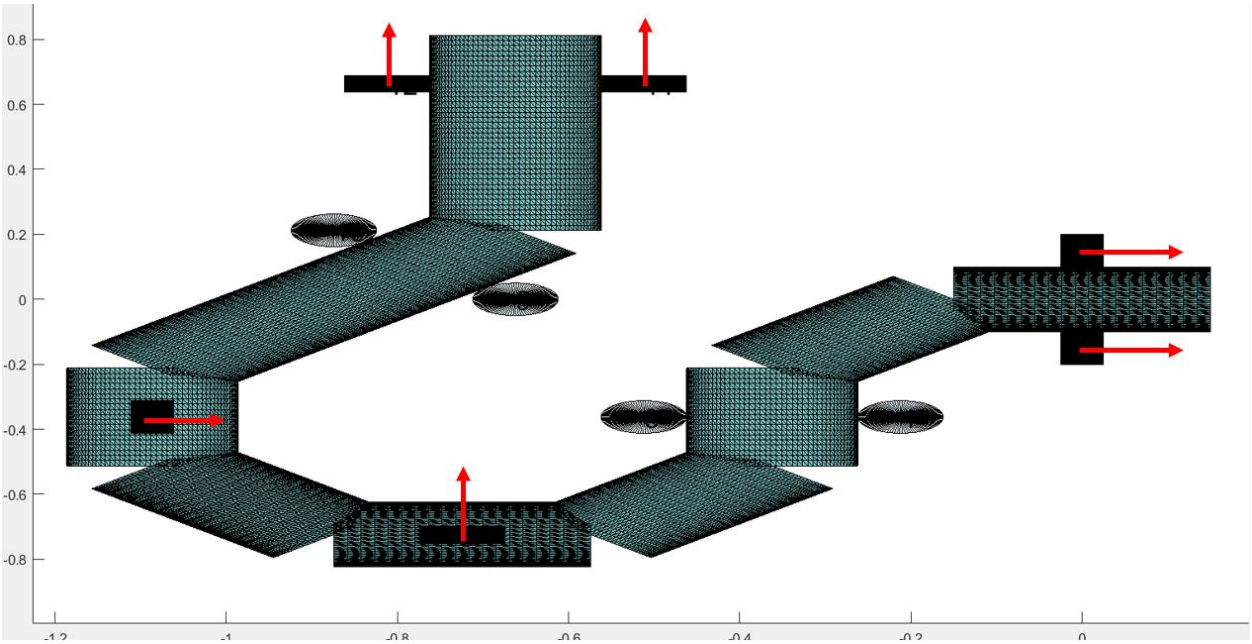

Figure 22 gamma shape

```
Matrix_A =

    1.0000    1.0000         0         0    0.0000    0.0000    1.0000    1.0000   -0.0000   -0.0000         0         0
         0         0    0.0000    0.0000    1.0000    1.0000   -0.0000   -0.0000   -0.0000   -0.0000   -1.0000   -1.0000
         0         0   -1.0000   -1.0000         0         0         0         0   -1.0000   -1.0000         0         0
         0         0    0.3621    0.3621   -0.1500    0.1500    0.0000   -0.0000    0.0000   -0.2121         0         0
         0         0   -0.5121   -0.2121    0.0000   -0.0000    0.1500   -0.1500   -0.6621   -0.8743         0         0
   -0.1500    0.1500   -0.0000   -0.0000   -0.7243   -0.7243    0.3621    0.3621    0.0000    0.0000    0.5121    0.8121


algorithm =

   16.0000
    0.0000
   16.0000
    0.2623
    5.1106
    0.3600


rank =

     3
```

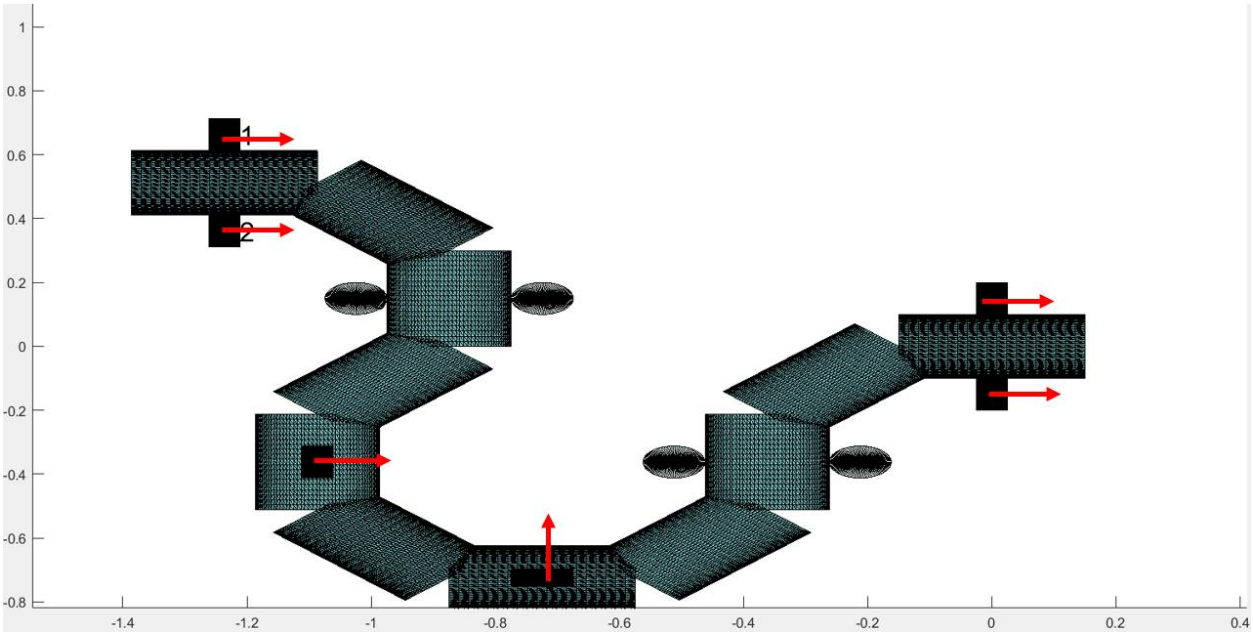

Figure 23 S shape

```
Matrix_A =

    1.0000    1.0000         0         0    0.0000    0.0000    1.0000    1.0000         0         0    1.0000    1.0000
         0         0    0.0000    0.0000    1.0000    1.0000   -0.0000   -0.0000   -0.0000   -0.0000         0         0
         0         0   -1.0000   -1.0000         0         0         0         0   -1.0000   -1.0000         0         0
         0         0    0.3621    0.3621   -0.1500    0.1500    0.0000   -0.0000   -0.1500   -0.1500         0         0
         0         0   -0.5121   -0.2121    0.0000   -0.0000    0.1500   -0.1500   -0.7243   -1.0243         0         0
   -0.1500    0.1500   -0.0000   -0.0000   -0.7243   -0.7243    0.3621    0.3621    0.0000    0.0000   -0.6621   -0.3621


algorithm =

   36.0000
    4.0000
   16.0000
    0.1800
    6.1147
    3.0574


rank =

     5
```

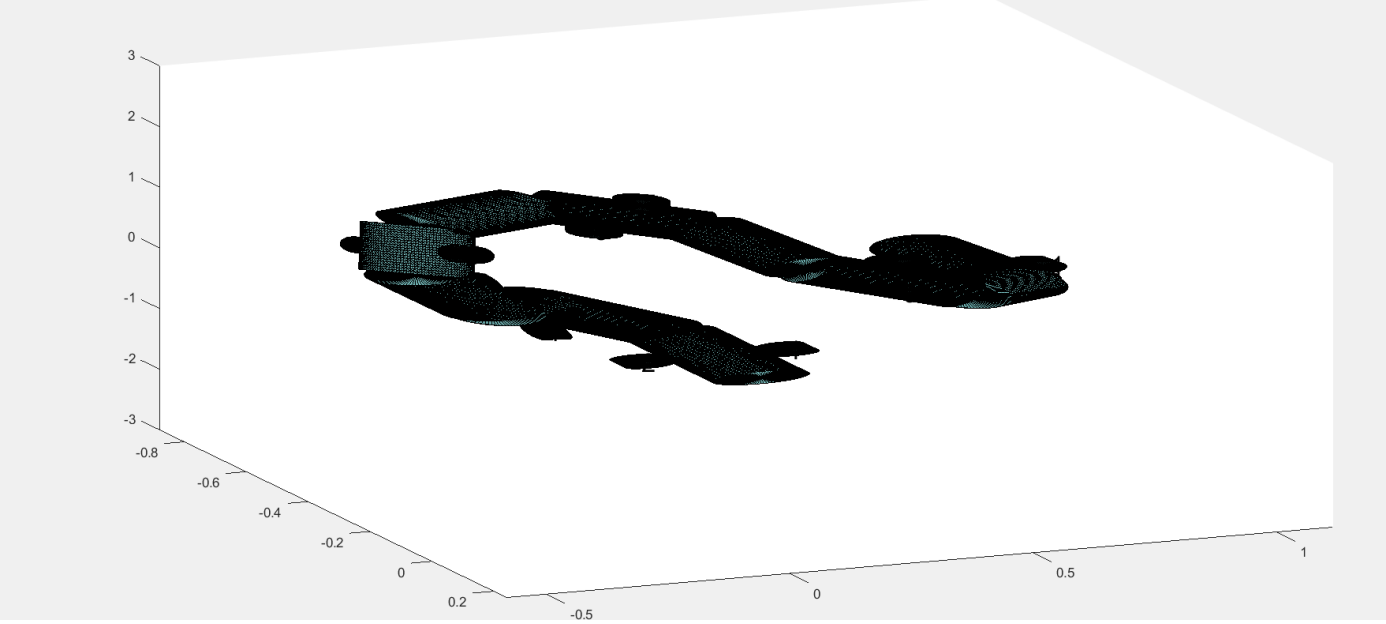

Figure 24 Random shape 1

```
Matrix_A =

    1.0000    1.0000   -0.2801   -0.2801    0.2608    0.2608    0.7963    0.7963    0.3376    0.3376    0.9321    0.9321
         0         0   -0.8679   -0.8679    0.8108    0.8108   -0.5046   -0.5046   -0.6991   -0.6991    0.0685    0.0685
         0         0   -0.4102   -0.4102   -0.5241   -0.5241    0.3337    0.3337   -0.6303   -0.6303    0.3558    0.3558
         0         0    0.4074    0.3109   -0.5522   -0.3207    0.5068    0.3293    0.2670    0.1004    0.2798    0.1756
         0         0   -0.2688   -0.1225    0.0092   -0.1412    0.8786    0.6495    0.2424    0.0358    0.3248    0.4596
   -0.1500    0.1500    0.2905    0.0470   -0.2606   -0.3780    0.1190    0.1963   -0.1259    0.0140   -0.7955   -0.5485


algorithm =

   37.1267
    5.6862
    3.0635
    2.2624
    4.2744
    2.0787


rank =

     6
```

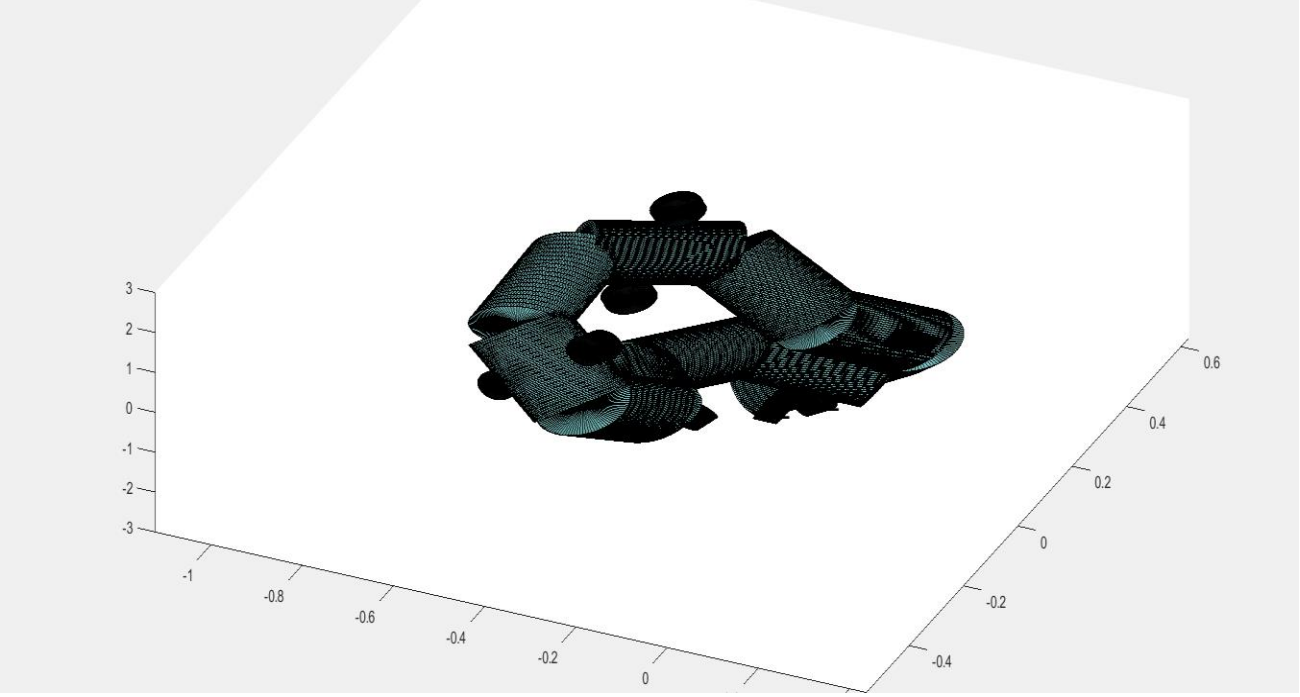

Figure 25 random shape 2

```
Matrix_A =

    1.0000    1.0000   -0.3184   -0.3184    0.4155    0.4155    0.4272    0.4272    0.0078    0.0078    0.6584    0.6584
         0         0   -0.9062   -0.9062    0.7154    0.7154   -0.4027   -0.4027   -0.9933   -0.9933    0.6418    0.6418
         0         0   -0.2782   -0.2782   -0.5618   -0.5618    0.8095    0.8095   -0.1149   -0.1149    0.3933    0.3933
         0         0    0.3974    0.2737   -0.4866   -0.2421    0.4613    0.1938    0.3725    0.1780    0.2263    0.0130
         0         0   -0.2271   -0.1081    0.1360   -0.0340    0.6392    0.5385    0.0215   -0.0062   -0.1784   -0.0709
   -0.1500    0.1500    0.2848    0.0388   -0.1866   -0.2224    0.0746    0.1656   -0.1609    0.0658   -0.0877    0.0939


algorithm =

   19.1905
    3.5730
    0.2460
    1.9250
    0.5049
    0.0043


rank =

     3
```

VIII. References

1. *Boulton, A. J., Humphreys, W. F., and Eberhard, S. M.: Imperiled subsurface waters in Australia: Biodiversity, threatening processes and conservation, 41–54,2003.*
2. *https://en.wikipedia.org/wiki/Karst.*
3. *Hydrogeologic Characterization and Methods Used in the Investigation of Karst Hydrology, Chapter 3 of "Field Techniques for Estimating Water Fluxes Between Surface Water and Ground Water", Charles J. Taylor and Earl A. Greene.*
4. *Lionel Lapierre. Aleyin: An underneath robotic journey – robotic systems for karst exploration. 2016.*
5. *https://en.wikipedia.org/wiki/Pozzo_del_Merro*
6. *British Sub-Aqua Club A review of the nature of diving in the United Kingdom and of diving fatalities in the period 1 st Jan 1998 to 31 st Dec 2009, Clare M. Peddie.*
7. *. Gray, "Studies in animal locomotion," Journal of Experimental Biology, vol. 10, no. 1, pp. 88–104, 1933.*
8. *S. Hirose, Biologically Inspired Robots: Snake-Like Locomotors and Manipulators. Oxford: Oxford University Press, 1993.*
9. *Kristin Ytterstad Pettersen, Jan Tommy Gravdahl, Pål Liljebäck, Øyvind Stavdahl, Snake Robots: Modelling, Mechatronics, and Control,2012.*
10. *McIsaac, K.A., Ostrowski, J.P.: Motion planning for anguilliform locomotion. IEEE Trans. Robot.Autom. 19(4), 637–652 (2003a)*
11. *Boyer, F., Porez, M., Khalil, W.: Macro-continuous computed torque algorithm for a threedimensional eel-like robot. IEEE Trans. Robot. 22(4), 763–775 (2006)*
12. *Zuo, Z., Wang, Z., Li, B., Ma, S.: Serpentine locomotion of a snake-like robot in water environment. In: IEEE Int. Conf. Robotics and Biomimetics, pp. 25–30 (2008)*
13. *Eleni Kelasidi, Kristin Ytterstad Pettersen, Jan Tommy Gravdahl,Modeling of underwater snake robots moving in a vertical plane in 3D,2014*
14. *E Kelasidi, KY Pettersen, JT Gravdahl, P Liljebäck, Modeling of underwater snake robots, 2014 IEEE International Conference on Robotics and Automation (ICRA), 4540-4547*
15. *P Liljebäck, Ø Stavdahl, KY Pettersen, JT Gravdahl, Mamba-A waterproof snake robot with tactile sensing, 2014 IEEE/RSJ International Conference on Intelligent Robots and Systems.*
16. *Eleni Kelasidi, Kristin Ytterstad Pettersen, Jan Tommy Gravdahl, A control-oriented model of underwater snake robots, 2014 IEEE International Conference on Robotics and Biomimetics (ROBIO 2014)*
17. *https://techacute.com/snake-robot-eelume-subsea-maintenance*
18. *Alireza Akbarzadeh, Design and Modeling of a Snake Robot Based on Worm-Like Locomotion,2011*
19. *Mohammadali Javaheri Koopaee, Design, Modelling and Control of aModular Snake Robot with Torque Feedback for Pedal Wave Locomotion on Surfaces with Irregularities,2019*
20. *Aksel Andreas Transeth , Kristin Ytterstad Pettersen, Developments in Snake Robot Modeling and Locomotion,2014*
21. *Thor I. Fossen, Svein I. Sagatun, LAGRANGIAN FORMULATION OF UNDERWATER VEHICLES, DYNAMICS, Division of Engineering Cybernetics,Norwegian Institute of Technology,NORWAY*